ADSORPTIVE REMOVAL OF PHOSPHATE ANION FROM AQUEOUS SOLUTION USING Al(III)- LOADED SAPONIFIED WATERMELON RIND

A DISSERTATION SUBMITTED TO THE

DEPARTMENT OF CHEMISTRY

AMRIT CAMPUS

INSTITUTE OF SCIENCE AND TECHNOLOGY

TRIBHUVAN UNIVERSITY

NEPAL

FOR THE PARTIAL FULFILLMENT OF REQUIREMENT OF

THE MASTER OF SCIENCE DEGREE IN CHEMISTRY

BY

SIRJANA BHATTARAI

SYMBOL NO: 2182/077

T. U. REGISTRATION NO.: 5-2-33-223-2016

JULY 2, 2024

BOARD OF EXAMINERS AND CERTIFICATE OF APPROVAL

The dissertation entitled 'Adsorptive removal of phosphate anion using Al(III)-loaded saponified watermelon rind' by **Ms. Sirjana Bhattarai** under the supervision of **Asst. Prof. Dr. Ram Lochan Aryal**, Department of Chemistry, Amrit Campus, Tribhuvan University, Kathmandu, Nepal, and under the co-supervision of **Asst. Prof. Dr. Deval Prasad Bhattarai**, Department of Chemistry, Amrit Campus, Tribhuvan University, Kathmandu, Nepal, hereby submitted has been approved for partial fulfillment of the requirement for completion of her Master of Science (M.Sc.) Degree in Chemistry. This dissertation has not been submitted to any other university or institution previously for the award of a degree.

.....

Supervisor

Asst. Prof. Dr. Ram Lochan Aryal

Amrit Campus,

TU, Kathmandu, Nepal

Tribhuvan University
Amrit Campus
Department of Chemistry

.....

Co-Supervisor

Asst. Prof. Dr. Deval Prasad Bhattarai

Amrit Campus

TU, Kathmandu, Nepal

.....

Internal Examiner

Assoc. Prof. Dr. Sharmila Pradhan

Amrit Campus,

TU, Kathmandu, Nepal

.....

External Examiner

Asst. Prof. Dr. Bhoj Raj Poudel

Tri-Chandra Multiple Campus

TU, Kathmandu, Nepal

.....

M.Sc. Chemistry Co-ordinator

Assoc. Prof. Dr. Bhushan Shakya

Department of Chemistry

Amrit Campus,

TU, Kathmandu, Nepal

.....

Head of the Department

Prof. Dr. Daman Raj Gautam

Department of Chemistry

Amrit Campus,

TU, Kathmandu, Nepal

July 2, 2024

LETTER OF FORWARD

Date:

On the recommendation of **Asst. Prof. Dr. Ram Lochan Aryal** and **Asst. Prof. Dr. Deval Prasad Bhattarai** the dissertation is submitted by **Ms. Sirjana Bhattarai** Symbol No. 2182/077, T.U. Registration No.: 5-2-33-223-2016 entitled **"Adsorptive removal of phosphate anion from aqueous solution using Al(III)-loaded saponified watermelon rind"** is forwarded by Department of Chemistry, Amrit Campus for the approval to the evaluation committee, Institute of Science and Technology (IoST), Tribhuvan University (T.U.), Nepal.

She has fulfilled all the requirements laid down by the Institute of Science and Technology (IoST), Tribhuvan University (T.U.), Nepal for the dissertation.

Tribhuvan University
Amrit Campus
Department of Chemistry

.....

Prof. Dr. Daman Raj Gautam

Head of Department

Department of Chemistry

Amrit Campus

TU, Kathmandu, Nepal

RECOMMENDATION

This is to recommend that **Sirjana Bhattarai**, (Symbol. No. 2182/077., T.U. Registration No. 5-2-33-223-2016), has carried out a dissertation entitled **"Adsorptive removal of phosphate anion using Al(III)-loaded saponified watermelon rind"** for the requirement to the dissertation in Master of Science (M.Sc.) degree in Chemistry under our supervision in the Department of Chemistry, Amrit Campus, Institute of Science and Technology (IoST), Tribhuvan University (T.U.), Nepal.

She has fulfilled all the requirements laid down by the Institute of Science and Technology (IoST), Tribhuvan University (T.U.), Nepal for the submission of the thesis for the partial fulfillment of the Master of Science (M.Sc.) degree in Chemistry.

Tribhuvan University
Amrit Campus
Department of Chemistry

.....

Supervisor

Asst. Prof. Dr. Ram Lochan Aryal

Department of Chemistry

Amrit Campus

Tribhuvan University

Kathmandu, Nepal

.....

Co-Supervisor

Asst. Prof. Dr. Deval Prasad Bhattarai

Department of Chemistry

Amrit Campus

Tribhuvan University

Kathmandu, Nepal

July, 2024

DECLARATION

This dissertation entitled **"Adsorptive removal of phosphate anion from aqueous solution using Al(III)-loaded saponified watermelon rind"** is being submitted to the Department of Chemistry, Amrit Campus, Institute of Science and Technology (IoST), Tribhuvan University (T.U.), Nepal for the partial fulfillment of the requirement to the dissertation in Master of Science (M.Sc.) degree in Chemistry. This dissertation is carried out by me under the supervision of **Asst. Prof. Dr. Ram Lochan Aryal** and co- supervision of **Asst. Prof. Dr. Deval Prasad Bhattarai** in the Department of Chemistry, Amrit Campus, Institute of Science and Technology (IoST), Tribhuvan University (T.U.), Nepal.

This work is original and has not been submitted earlier in part or full in this or any other form to any university or institute, here or elsewhere, for the award of any degree.

.....

Sirjana Bhattarai

Symbol No: 2182/077

T. U. Registration No.: 5-2-33-223-2016

ACKNOWLEDGEMENTS

I feel immense pleasure in acknowledging my heartfelt sense of gratitude to my respected supervisor **Asst. Prof. Dr. Ram Lochan Aryal** Department of Chemistry, Amrit Campus and my co-supervisor **Asst. Prof. Dr. Deval Prasad Bhattarai** for their sustained encouragement, regular guidance, inspiration, valuable suggestion, and great support throughout my working period.

My deepest gratitude goes to the Head of the Department, **Prof. Dr. Daman Raj Gautam**, and M.Sc. Chemistry Co-ordinator **Assoc. Prof. Dr. Bhushan Shakya**, Amrit Campus for providing all the lab space required for this research as well as their gracious suggestions.

I would like to extend my heartfelt thanks to my esteemed lecturers for their invaluable advice and assistance throughout the research phase. I am deeply grateful to the lab representatives, **Mr. Mani Raj Budhathoki** and **Mr. Nanda Krishna Manandhar**, for their crucial support in the success of this research project.

Lastly, I express my sincere gratitude to my family, friends Niranjan Ghimire, Sujan Dhital, Sarmila Dangi, Puja Thanaït, Susmita Panthi and brother Pukar Bhattarai for their constant support and encouragement.

SIRJANA BHATTARAI

July 2, 2024

ABSTRACT

A primary factor in the eutrophication and deterioration of water bodies is high phosphate content, which is frequently caused by NPK fertilizers. Modified watermelon rind has ability for water treatement. In this study, watermelon rind was grinded with a grinding mill, washed with distilled water and saponified with $Ca(OH)_2$ resulting the preparation of saponified watermelon rind (SWR) and then treated with Al(III) to develop effective biosorbent which is called aluminium loaded saponified watermelon rind abbreviated as Al(III)-SWR. The extraction was believed to be done by ligand and ion exchange processes. The polymeric constituent was revealed by FTIR plot. The point of zero charge (pHpzc) of the biosorbents was found to be 4.05. The capacity to remove phosphate relies on various parameters like pH, initial concentration, contact time, and adsorbent dosages. Using Al(III)-SWR, the maximum phosphate adsorption was observed 18.25% at pH 1.78 to a maximum of 87.91% at pH 3.91. The maximum phosphate adsorption capacity of phosphate was found to be 15.95 mg/g. Both the Langmuir isotherm and pseudo second order (PSO) kinetic model were found to be accurately represented through the experimental data. These results highlight the potential of Al(III)-SWR as a highly effective adsorbent for phosphate ion removal from aqueous solutions.

Keywords: Watermelon rind, Al(III)-SWR, adsorption, phosphate anion

शोध सार

जलस्रोत, पारिस्थितिक प्रणाली र मानव स्वास्थ्यमा एनायोनिक (anionic) प्रदुशकहरुले प्रतिकूल प्रभाव पारेको छ जसमा मुख्यरूपमा फोस्फेट पाइएको छ। माटोमा दुई किसिमको फोस्फेट, जैविक र खनिज फोस्फेट पाइन्छन्। परिमार्जित खरबुजाको बोक्रामा उक्त प्रदूषक हटाउने क्षमता हुन्छ त्यसैले खरबुजाको बोक्रालाई राम्ररी पखालेर, सुकाएर, ग्राइन्डरमा पिसेर धुलो तयार पारियो। त्यसपछि उक्त धूलोलाई सेपोनिफिकेसन (saponification) गरेर Al(III) ले treatment गरियो। लिगान्ड र आयन exchange प्रक्रियाहरू मार्फत, कार्बोक्सिल फंक्शनलाइजेसनका साथ यी एड्जर्प्सनहरूले प्रभावकारी रूपमा पानीबाट फस्फेट आयनहरू निकाल्ने कुरा अध्यायन गरियो । कार्यात्मक समूहहरूको गर्नको लागि फोरियर ट्रान्सफर्म इन्फ्रारेड स्पेक्ट्रोस्कोपी (FTIR) विधिद्वारा अध्यायन गरियो । एड्जर्वेन्टको शून्य चार्ज (pHpzc) 4.0 पीएच (pH) बिन्दु मा फेला पर्यो । फोस्फेट हटाउने क्षमता पीएच, एकाग्रता, कन्ट्याक टाईम (contact time) र एड्जर्वेन्टको डोज सहित विभिन्न प्यारामिटरहरूमा निर्भर रहेर अध्यायन गरियो । Al(III)-SWR प्रयोग गरेर, अधिकतम फास्फेट एड्जर्प्सन pH 3.91 मा अवलोकन गरियो र साथै अधिकतम फोस्फेट एड्जर्प्सन क्षमता 15.95 mg/g रहेको अध्यायन गरियो । Langmuir isotherm model र pseudo second order (PSO) काइनेटिक मोडेलले प्रयोगात्मक डाटालाई सही रूपमा प्रतिनिधित्व गरेको पाईयो । यी नतिजाहरूले Al(III)-SWR को जलीय समाधानबाट फस्फेट आयन हटाउनको लागि अत्यधिक प्रभावकारी एड्जर्वेन्टको रूपमा प्रस्तुत गर्दछ।

शब्दकुञ्जीका : एड्जर्प्सन, खरबुजाको बोक्रा, फोस्फेट आयोन, सपोनिफिकेशन

LIST OF ACRONYMS AND ABBREVIATIONS

RWR	Raw watermelon rind
SWR	Saponified watermelon rind
Al(III)-SWR	Aluminium loaded SWR
ppm	Parts per million
mg/g	Milligram per gram
mol/kg	Molecules per kilogram
mg/L	Milligram per liter
rpm	Rotation per minute
C_i	Initial concentration
C_e	Equilibrium concentration
g/L	Gram per liter
FTIR	Fourier transformed infrared spectroscopy
%Ad.	Percentage biosorption
k_1	Pseudo-first-order rate constant
k_2	Pseudo-second-order rate constant
q_e	Amount biosorbed at equilibrium
q_t	Amount biosorbed at time
q_m	Maximum adsorption
UV-Vis	UV visible spectrophotometer
min.	Minute
nm	Nanometer
T%	Percentage transmittance

LIST OF SYMBOLS

%	Percentage
λ_{max}	Maximum wavelength
R^2	Coefficient of determination
K	Kelvin scale
Δ	Delta
&	And
m	Mass of the adsorbent
v	Volume of the solution

LIST OF SCHEMES

LIST OF TABLES

LIST OF FIGURES

TABLE OF CONTENTS

CHAPTER-1
INTRODUCTION

1.1. Background

Water is essential for all living organisms on earth and is crucial for human survival. It is essential for maintaining basic human processes like digestion, breathing, blood circulation, elimination of waste, and reproduction (Kılıç *et al*., 2020). The Earth's hydrosphere is supposed to contain a huge amount of water, roughly 1386 million cubic kilometers (km^3). Nevertheless, only 2.5 % is freshwater; roughly 97.5 % is saltwater and within this fraction of fresh water, lakes and rivers include 1.3 %, groundwater makes up 30 %, and ice and glaciers contain 68% of it (Sartor & Boyd, 1972). Particularly freshwater is vital to life and serves important functions in homes, businesses, and agriculture (L′vovich *et al*., 1979).

Water resources contain a variety of pollutants, including anions, heavy metals, and non-metals, which are caused by both natural processes and human activities (Saravanan *et al.*, 2021). Both human health and aquatic ecosystems are seriously affected by these pollutants (EKhaiary *et al*., 2011). Pollution of groundwater, which comes from a variety of sources such as industrial effluents, unmanaged buildings, and waste disposal sites are the major worldwide issues (Madhav *et al.*, 2020). Around 100 million tons of garbage are generated from hundreds of thousands of affected places worldwide (Shiklomanov *et al*., 2003). Numerous countries have taken action in response to the global problem of phosphate contamination; Switzerland is one of them that has gone so far as to outlaw the use of phosphate in detergents (Schaum, 2018).

As an essential component of DNA, RNA, ATP, and phospholipids, an anionic pollutant, phosphate involves a number of metabolic activities (Divya Jyothi *et al*., 2012). But phosphate is extremely dangerous for human health and aquatic life. Phosphate can be harmful even in small amounts in water (Schwarzenbach *et al.* 2010). The World Health Organization (WHO) recommends that phosphate levels in drinking water should be below 1.5 mg/L to ensure safety and prevent health issues. Phosphates are found in water (aquatic ecosystems, including lakes and rivers), air and soils originated from industrial effluent, agricultural runoff (pesticides, herbicides, and fertilizers), vehicles, mining, cosmetics and electronic devices (Amin *et al*., 2014, Lin *et al*., 2022). When phosphate concentrations are higher than 0.2 mg/L, they may promote the growth of algae and

plants, which can cause eutrophication and oxygen loss (Schindler *et al.*, 1971). Eutrophication occurs in water areas like lakes, ponds, streams and rivers when phosphorus dissolved in wastewater combines with runoff from various other sources (Smith & Schindler, 2009). This leads to algal blooms that lower oxygen levels and affect the condition of aquatic ecosystems by degrading water quality parameters (Manna *et al.*, 2022). Overall, Increased phosphate levels that cause eutrophication in rivers encourage the growth of algae, which when broken down by microorganisms reduces the amount of dissolved oxygen in the water, making the river unsuitable for aquatic life and possibly resulting in anaerobic conditions, color changes, decreased mineral stability, and foul odors (Badamasi *et al.*, 2019).

High levels of phosphate (PO_4^{3-}) can have various adverse effects, prompting the need to remove or decrease phosphorus (P) from wastewater and recover it to mitigate environmental damage (Li *et al*., 2016). Because of variables including pH and ionic strength, phosphorus can be found in water in a variety of orthophosphate anions (Holtan *et al*., 1988). In an aqueous solution, phosphate is present in various oxo-anions, including PO_4^{3-} (phosphate), HPO_4^{2-} (hydrogen phosphate), $H_2PO_4^-$ (dihydrogen phosphate), and H_3PO_4 (phosphoric acid) (Pokhrel *et al*., 2019). The existence of various forms of phosphate is necessary to know for the suitable treatment technologies (Poudel *et al*, 2020). The dissociation of phosphate anion in aqueous solution occurs in three steps, each with its own equilibrium constant which indicates the pH at which the species are in equilibrium. It can be presented as,

$$H_3PO_4 \longrightarrow H^+ + H_2PO_4^- \qquad pKa_1 = 2.12$$

$$H_2PO_4^- \longrightarrow H^+ + HPO_4^{2-} \qquad pKa_2 = 7.21$$

$$HPO_4^{2-} \longrightarrow H^+ + PO_4^{3-} \qquad pKa_3 = 12.36$$

The dissociation of orthophosphoric acid begins as soon as the pH of the solution increases above the value of 2.12, where it starts losing its hydrogen ion and converted into dihydrogen phosphate. The dihydrogen phosphate remains predominant below pH 7.21, above which it starts losing its proton forming hydrogen phosphate. At, pH 7.21, there is equilibrium where half of the dihydrogen phosphate is dissociated into hydrogen phosphate and becomes dominant until below pH 12.36. At the pH 12.36, hydrogen phosphate and phosphate ions maintain its equilibrium. The phosphate ion concentration increases gradually and reaches its top at around pH 14.

The pH of the aquatic environment determines the forms in which Orthophosphate (PO_4^{3-}) ions can appear in multiple ionic species.

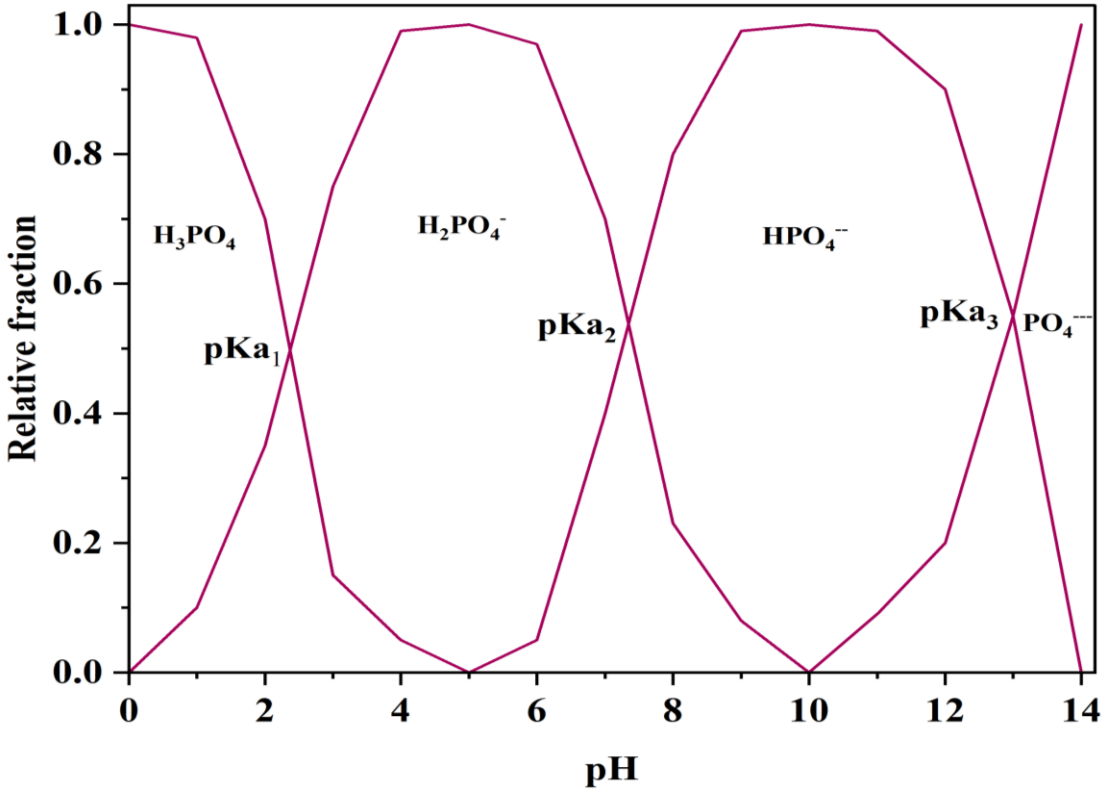

Figure 1: Distribution diagram of phosphate at different pH (Currie *et al*., 2017)

At a pH of around 0-2, H_3PO_4 is the predominant species, accounting for nearly the 100 % of the phosphate. As the pH increase to around 2-7, $H_2PO_4^-$ becomes the dominant species reaching almost 100 % around pH 4. Between pH 7-12, HPO_4^{2-} is the predominant species, showing its peak near 100 % around pH 9. At pH level above12, PO_4^{3-} becomes the dominant oven other species of the phosphate approaching 100 % near pH 14.

1.2. Different methods for phosphate removal

Different conventional methods have been operated to adsorb phosphate from contaminated water through membrane separation technologies (Guoqiang *et al*., 2023), chemical oxidation and reduction (Dixit *et al*., 2021) , precipitation (Caporali *et al*., 2021), co-precipitation (Besenhard *et al*., 2020) evaporative recovery (Ma *et al*., 2022) , electrochemical treatment (Rodriguez *et al*., 2022) and reverse osmosis (Peleka & Deliyanni, 2009) etc. These adsorption technologies have several demerits, including high operational costs, limited adsorption capacity, slower kinetics, and disposal issues of used

adsorbents, lack of selectivity, surface fouling, and significant energy consumption during regeneration**.** In this context, adsorption is considered the most effective technique for removing anions from water bodies, as it is cost-effective, simple to implement, highly efficient, and capable of handling low contaminant concentrations without generating significant waste, with the added benefit that adsorption materials can often be regenerated and reused, reducing environmental impact and operational expenses (Blaney *et al*., 2007).

1.3. Low Cost adsorbents and its importance

The various methods to remove phosphate from aqueous solution include: micro algal biofilms, precipitation combined with filtration (sand filtration or ultrafiltration), chemical precipitation, crystallization technology, ion exchange etc. (Peleka & Deliyanni, 2009). However, questions remain regarding these technologies, particularly concerning economic viability and social acceptability. Therefore, adsorption is among the most common and efficient methods for eliminating hazardous pollutants from wastewater.

Adsorbents based on biomaterials, often called bio-adsorbents have been studied as cost effective and environmentally favorable means to remove pollutants. Environmentally friendly and economically viable methods of pollutant removal have been investigated for biomaterial-based adsorbents, called bio-adsorbents. Lignocellulosic waste from forestry and agriculture is gaining attention as a cost-effective bio-adsorbent for removing toxicity of anions from water. Palm kernel fibers (Ofomaja *et al*., 2007), coir pith (Sarkar *et al*., 2021), banana pseudo stem fibers (Silva *et al*., 2021), rice husk (Alver *et al*., 2020), peanut hull (Aryee *et al*., 2021), tea waste (Çelebi *et al*., 2021), wheat husk(Franco *et al*., 2021), rubber, seed coats, sugarcane bagasse etc. are some example of agro waste that have been employed to eliminate phosphate (Saravanan *et al*., 2021).

For my dissertation, I used the rind of watermelon, which is one of the most widely available and affordable fruits in South and Southeast Asia, with an average annual production of 350,000 tons. (Ahmadi *et al*,. 2017). With this data, the use of watermelon rind as bio-adsorbent is reasonable.

Watermelon rind contains non-essential amino acids, citruline, carotenoids, protein, cellulose and pectin rich in functional groups like: -OH(cellulose), -COOH(pectin), -NH_2 (pectin) etc. (Romdhane *et al.*, 2017). Percent distribution of pectic acid in watermelon

rind is the highest compared to other polysaccharides and thus adsorbent in this study was designed considering pectin content (R. MD. *et al.*, 2019).

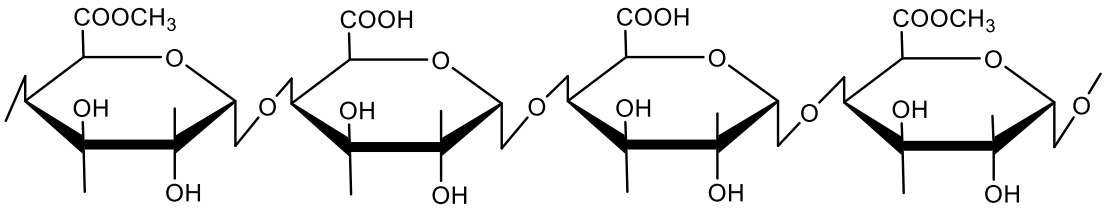

PECTIN

Scheme 1*:* Chemical structure of pectin

Pectic acid partially undergoes methyl esterification to produce an acidic polymer, pectin acid salt. It has high affinity for trivalent metal ion like Al(III). In this work, RWR was treated with $Ca(OH)_2$ to saponify the methyl groups and was later loaded with trivalent Al(III) to prepare desired adsorbent.

Figure 2: Watermelon fruit

Transitional metal loading produces positively charged metal ions appropriate for retaining negatively charged anions like phosphate. Therefore, metal loading into bio sorbents is a preferred method since it is quick, effective, and increases affinity for phosphate ions (Nguyen *et al.*, 2014).

1.4. Adsorption

Adsorption is the process by which atoms or molecules from a gas or liquid stick to the surface of a solid or liquid to produce a thin layer. This phenomenon occurs due to the mutual attraction between the surfaces of the adsorbent and adsorbate (Szilagyi *et al.*, 2014). Adsorption emerges as a preferable choice for waste elimination owing to its capability to effectively regenerate and recover adsorbed substances, facilitating their

reuse. Adsorption can be categorized into two primary types depending on the intensity of the bond formed between the adsorbate and adsorbent (Sing, 1998).

1.4.1. Physical Adsorption (Physisorption)

Physical adsorption happens when molecules of the adsorbate adhere to the surface of the adsorbent and occurs via relatively weak van der Waals forces, including dispersion forces and dipole-dipole interactions and is often reversible, influenced by surface area, temperature, and pressure, typically occurring at lower temperatures and across diverse surface types (Hill, 1952).

1.4.2. Chemical Adsorption (Chemisorption)

Chemical adsorption entails a more potent interaction between the adsorbate and adsorbent, frequently leading to the creation of chemical bonds, which are typically irreversible and involve electron exchange or sharing, characterized by specificity, selectivity, and higher activation energy compared to physical adsorption, often occurring at elevated temperatures on surfaces with active sites or functional groups capable of forming chemical bonds (Jing *et al*., 2017).

Physical and chemical adsorption represent opposite ends of the adsorption spectrum, but real-world systems often display a blend of both, influenced by factors like adsorbate properties, adsorbent surface characteristics, and operating conditions (Borukhov *et al*., 1999). Biosorption is a suitable approach for PO^{4---} treatment due to its equal success in eliminating both organic and inorganic contaminants (Breeuwsma & Lyklema, 1973).

1.4.3. Biosorption

Biosorption is the process by which dead or living biological components adsorb pollutants, including heavy metals, from aqueous solutions. It is a highly accepted alternative for treating industrial wastewater and cleaning up contaminated areas because of its affordability, effectiveness, and environmental friendliness. It is a sustainable method where biological materials, like watermelon rinds, are used to remove pollutants from water. When water containing pollutants comes into contact with watermelon rind, the pollutants are attracted to and adhere onto the surface of the rind, effectively removing them from the water. This eco-friendly approach offers a cost-effective and efficient way to purify water, making use of readily available agricultural waste materials like watermelon rinds to address environmental pollution concerns.

1.5. Ligand exchange mechanism

Ligand exchange in phosphate adsorption is a process where phosphates in solution replace ligands (hydroxyl groups) that are initially bound to the adsorbent's surface. This mechanism is also common in adsorption involving oxides and hydroxides of metals, such as alumina or iron oxides. In this process, the anion forms a strong bond with the surface metal atoms, displacing the original ligands. Ligand exchange is particularly effective for adsorbing anions like phosphate, arsenate, and sulfate, as these anions can form stable complexes with the surface metal ions, enhancing the adsorption capacity and specificity of the adsorbent.

1.6. Factors affecting adsorption

The adsorption is greatly affected by the starting concentration of the adsorbate, pH, the mass of the adsorbent, and the duration of the adsorbent-adsorbate contact time in batch studies. The effect of these parameters on adsorption process will be studied by varying one of the factors while keeping others constant (Weng *et al*., 2012).

1.6.1. Effect of pH

As pH rises, the ability of anion to adsorb onto an absorbent increase due to the increase of negatively charged surface groups. By enticing metal cations, a higher pH causes more active functional group sites to be free and exposed (negative charge) and less H^+ ion present, which improves adsorption. On the other hand, when pH decreases, the ability of metal and non-metal anions to be adsorbed increases because of a rise in the adsorbent's positively charged surface functional groups (Aryal & Liakopoulou 2011).

1.6.2. Effect of adsorbent dosage

As the adsorbent dosage is increased, the percentage of metal and non-metal ions removed during adsorption rises while the equilibrium adsorption capacity falls. Conversely, a decrease in adsorption capacity with higher bio sorbent dose may be caused by the adsorption medium & severe restrictions on the mobility of ionic species, which leads to unsaturation of some attachment sites during the adsorption process (Lakshmipathy & Sarada, 2013).

1.6.3. Effect of contact time

The specific surface area of biomass is closely related with the adsorption of metals or non-metals. The surface area can be expanded by reducing biomass into a finer powder

form. The larger surface area of the biomass will expose more surface binding sites, enhancing adsorption and reducing contact time (Habiby *et al*., 2020).

1.6.4. Effect of initial concentration

It is clear that raising adsorbate ion concentration increases adsorbed ions per unit mass of adsorbent because the initial adsorbate concentration provides the necessary energy to break through the barrier to adsorbate the mass transfer of ions between the solid and aqueous phases. The adsorption capacity may increase with concentration due to the improved interactions between the adsorbate metal and non-metal ions (M. Aryal & Liakopoulou-Kyriakides, 2011).

1.7. Adsorption studies

The performance of the adsorbent in the adsorption process is analyzed by batch adsorption studies. Finding the ideal parameters to maximize the adsorption capacity of adsorbent is a valuable outcome of this work. The reaction pathway and adsorption process mechanism can be extracted by the examination of different parameters. Changes in solution pH, adsorbent dosage, contact times, initial ion concentration in the solution, and other factors are all used to study the adsorption capacity of synthesized adsorbents (Ajmal *et al*., 2003). Predefined volume of solution with varying concentrations of adsorbate is combined with a predetermined amount of adsorbent in batch adsorption investigations. Next, this combination is put in a rotatory incubator shaker and given a whole day to reach the ideal pH through equilibration. The initial concentration of the adsorbate is ascertained after this equilibration period, and centrifugation is then used to estimate the concentration that remains in the solution following adsorption.

The adsorption efficiency (A%) and the amount of adsorbate absorbed per gram of adsorbent (q_e) are measured in all tests using a constant mass balance relationship. The degree to which adsorbate molecules have stuck to the adsorbent's surface can be measured with the use of this relationship.

$$q_e = \frac{(C_i - C_r)V}{m} \quad (1)$$

$$A\ (\%) = \frac{(C_i - C_r)}{C_i} \times 100\ \% \quad (2)$$

Where, C_i is initial concentration and C_r is residual concentration of adsorbate in the solution (mg/L), V denotes volume of adsorbate solution (in L) and m is the mass of adsorbent (g).

1.8. Adsorption kinetics

Adsorption kinetics examines the sequestration of adsorbate from the solution and provides accurate details on the mechanism of adsorption in the batch process, which focuses on the removal of the pollutant in two phases: first, a quick removal phase, and then a gradual phase leading to equilibrium. The effectiveness of the adsorption process is determined by the rate at which adsorbates are absorbed by bio sorbents, which also determines the adsorption kinetics (Nagoya *et al.*, 2019a).

1.8.1. Pseudo first order (PFO) model

The pseudo-first-order model, developed by Lagergren (1898), describes the kinetics of adsorption processes. It assumes that the rate of occupation of adsorption sites is directly proportional to the number of unoccupied sites. This model is typically used to describe the initial stage of adsorption where the rate of adsorbate uptake is proportional to the difference between the equilibrium concentration and the amount adsorbed at any time. Despite its utility in predicting the early phase of adsorption, it often does not accurately forecast the adsorption behavior over longer periods. The pseudo-first-order model is mathematically expressed as a differential equation and its integrated form is commonly used to fit experimental data.

The non-linear form of PFO can be represented as:

$$q_t = q_e(1 - e^{-k_1 t}) \quad (3)$$

On representing equation (3) into linear form, it can be written as,

$$\log (q_e - q_t) = \log q_e - \frac{k_1}{2.303} t \quad (4)$$

Here, the amount of adsorbate adsorbed per unit weight of the adsorbent at equilibrium and at a specific time 't' are represented by 'qe' and 'qt' respectively, both measured in

mg/g. The PFO rate constant, 'k_1' (1/min), as well as 'q_e', can be calculated from the slope and intercept of the graph of $\log(q_e - q_t)$ plotted against time 't' (Panda *et al*., 2017).

1.8.2. Pseudo second order (PSO) model

The Pseudo-Second Order (PSO) model is essential for analyzing adsorption kinetics, particularly in removing pollutants from water. It often provides a better form to experimental data compared to the Pseudo-First Order (PFO) model. The PSO model indicates that the adsorption process is primarily driven by chemisorption, involving electron sharing or exchange between the adsorbent and adsorbate, helping to predict the adsorption capacity and efficiency of various materials (Ho & McKay, 1998; Blanchard *et al.*, 1984).

In its non-linear form, PSO can be expressed as,

$$q_t = \frac{q_e^2 . k_2 t}{q_e k_2 t + 1} \qquad (5)$$

On rearranging, above equation can be expressed as;

$$\frac{t}{q_t} = \frac{1}{k_2 q_e^2} + \frac{1}{q_e} t \qquad (6)$$

Where, the PSO rate constant is denoted as "k_2" in g/(mg min. Plotting 't/q_t' against 't' yields a linear relation that helps in the determination of 'q_e and 'k_2' using the slope and intercept, respectively (El-Khaiary & Malash, 2011).

1.9. Isotherm studies

The amount of adsorbate per unit mass of adsorbent as a function of the concentration of adsorbate still present in the solution at equilibrium at constant pH and temperature is represented graphically by an isotherm. Understanding the mechanism of adsorption, clarifying the biosorbent's adsorption capacity, and interpreting the way the adsorbent interacts with the adsorbate are all made easier with the help of isotherm studies. Models of the Freundlich and Langmuir isotherms are frequently used to explain adsorption processes.

1.9.1. Langmuir isotherm model

The Langmuir isotherm is a fundamental model in adsorption science. It assumes that adsorption occurs in a monolayer on a surface with uniform and energetically equivalent sites. It proposes that once a site is occupied, no further adsorption can take place at that

site. This model implies that adsorption is a reversible process and that there is no interaction between adsorbate molecules once they are adsorbed onto the surface. The Langmuir isotherm equation is widely used to describe adsorption phenomena, particularly in systems where adsorbate-adsorbent interactions are relatively simple and well-defined.

The nonlinear expression of the Langmuir isotherm model is defined by the following equation (Langmuir, 1918);

$$q_e = \frac{q_m b C_e}{1 + b C_e} \qquad (7)$$

We can convert the Langmuir isotherm equation into a linear form, which is shown as follows;

$$\frac{C_e}{q_e} = \frac{1}{q_{max} b} + \frac{C_e}{q_{max}} \qquad (8)$$

Where, 'q_e' represents the adsorption capacity at equilibrium, measured in milligrams per gram (mg/g), 'C_e' represents the equilibrium concentration in milligrams per liter (mg/L). The parameters 'b' and 'q_m' represent the equilibrium constant and the maximum adsorption capacity at monolayer, expressed in mg/g and liters per milligram (L/mg) respectively and determined by analyzing the slope and intercept of the linear correlation between C_e/q_e and C_e (Mittal *et al.*, 2009).

1.9.2. Freundlich isotherm model

The Freundlich isotherm model suggests that adsorbate molecules attach in multiple layers to a heterogeneous adsorbent surface, with varying energy levels at different binding sites. This model implies that the adsorbent surface remains unsaturated, allowing for unlimited surface coverage, indicating physisorption.

The non-linear equation for the Freundlich isotherm is expressed as follows (Freundlich, 1906).

$$q_e = K_F C_e^{1/n} \qquad (9)$$

The linear form of equation (10) can be derived by applying the natural logarithm as follows;

$$\log q_e = \log K_F + \frac{1}{n} \log C_e \quad (10)$$

where, 'C_e' (mg/L) and 'q_e' (mg/g) represent the equilibrium concentration and biosorption capacity, respectively. The Freundlich biosorption constant, 'K_F' (mg/g) $(L/mg)^{(1/n)}$ indicates the maximum biosorption capacity of the biosorbent, while '1/n' is a dimensionless parameter representing the heterogeneity of the biosorbent surface. The biosorption process is considered more favorable when '1/n' values fall between 0.1 and 1 (Shi et al., 2009). By plotting log q_e against log C_e, a straight line is obtained, from which '1/n' and 'K_F' can be determined. The slope of the line corresponds to '1/n', and the intercept corresponds to log K_F. The biosorption process is deemed favorable when $0 < 1/n < 1$, and unfavorable when $1/n > 1$ (Ren *et al.*, 2018).

1.10. Different methods for determination of phosphate concentration

Several methods are at hand for determining phosphate (PO_4^{3-}) concentration in liquid mediums like soil or water, each with its own strengths suitable for varying concentration levels. While traditional methods such as titrimetry and complex-gravimetry are effective for higher concentrations, colorimetry, atomic absorption spectroscopy (AAS), flow injection analysis (FIA), High-performance liquid chromatography (HPLC), ion chromatography (IC), and inductively coupled plasma atomic emission spectroscopy (ICP-AES) are highly effective techniques for detecting low concentrations of phosphate. However, the method choice depends on factors like sensitivity, sample complexity, and available resources. For routine analyses, simpler and cost-effective techniques like colorimetry or FIA may suffice, while more sophisticated methods like HPLC or ICP-AES might be utilized for specialized purposes.

1.11. Objective of the study

1.11.1. General objective

The general objective is the preparation of an anion exchange type adsorbent from the natural biopolymer of watermelon rind and to study the adsorption performance of Al(III)-loaded watermelon rind for the removal of phosphate anion from aqueous solution.

1.11.2. Specific objectives

The following are the specific goals of this research work;

- Functionalization of the adsorbent loaded with Al(III) followed by saponification.
- Characterization of adsorbents using FTIR analysis.

- Estimation of functional group in SWR by Boehm titration.
- Investigation of the adsorption capacity of Al(III)-loaded adsorbents in batch mode.
- Computation of kinetics and isotherm studies of adsorption process.
- Comparison among the adsorbents for their adsorption capacity with those found in the literature.

CHAPTER-2
LITERATURE REVIEW

2.1. Literature review

A survey indicates that there has been considerable global research focused on the removal of phosphate from water. Among the methods explored, adsorption stands out for its cost-effectiveness, convenience, and environmental friendliness. Particularly, the use of chemically modified agricultural waste for phosphate adsorption has recently gained attention as a promising and environmentally advantageous alternative.

The iron-loaded pomegranate peel (IL-PP) was characterized through zeta potential measurement, scanning electron microscopy, and Fourier transform infrared analysis. By employing the batch adsorption method, the equilibrium time and pH effect on the adsorption process were determined. A full factorial design methodology was used to analyze the effects and interactions of influencing parameters. The process effectively removed up to 90 % of phosphate within 60 minutes at pH 9 and 25 °C using a 150 mg dose of IL-PP. Non-linear modeling was applied for isotherm and kinetics analysis, revealing that the kinetics best fit the Elovich model ($R^2 = 0.97$), indicating chemisorption dominance, while the isotherm conformed to both Langmuir ($R^2 = 0.98$) and Freundlich ($R^2 = 0.94$) models, with a maximum phosphate uptake of 49.12 mg/g (Bellasen *et al*., 2021).

The phosphate ion results revealed that Zr(IV)-SWR exhibited a maximum biosorption capacity of 27.65 mg/g, while Zr(IV)-SBP displayed a capacity of 36.02 mg/g for phosphate ions. Also for fluoride ions, Zr(IV)-SWR demonstrated a maximum biosorption capacity of 28.98 mg/g, while Zr(IV)-SBP exhibited a capacity of 36.02 mg/g. The desorption process indicated that base solution (2M NaOH) was effective for fluoride ion desorption. The adsorption process was found to follow the Langmuir isotherm model and the pseudo-first-order model (Aryal *et al*., 2021).

In a study by Cheng *et al*., (2023), where phosphate adsorbent was prepared using a simple hydration method with industrial material, achieving an adsorption capacity of 3.27 mg P/g at a low phosphate concentration of 0.1 mg P/L. The adsorption process primarily involved ligand exchange and surface precipitation. In fixed-bed tests, the adsorbent demonstrated high removal efficiency with an empty bed contact time (EBCT) of just 1.18 minutes. The fixed-bed column adsorption performance demonstrated that

CAH_{10} could effectively remove phosphate from real secondary effluent and achieve a low concentration of 0.1 mg P/L.

The elimination of phosphate from aqueous solutions by zero-valent iron (ZVI) was studied in detail. Efficiency of phosphate removal was significantly impacted by solution pH. When the pH was raised from 3 to 4.5, the elimination of phosphate reduced from 96.4 to 48.4 % and then increased as the pH was raised further. At pH 7, the highest elimination effectiveness of 97.3 % was attained. When the pH was more than 7, the removal efficiency declined as the pH rose. The elimination of phosphate was significantly reduced to 8.6 % at pH 11. ZVI performed phosphate removal via adsorption and precipitation in the pH range of 3 to 11 with average relative deviations of 7.3 and 15.1 %, respectively (Nagoya *et al*., 2019).

The mango fruit (*Magnifera indica*) pectin-enriched biomass was used to make the natural anion exchanger, which was then loaded with trivalent iron, or Fe(III), to remove phosphate from water. Elements analysis and methods for identifying functional groups were used to characterize the adsorbent. The outcome showed that changing the pH value allowed for simple regulation of the phosphate adsorption utilizing Fe(III)-SMW. Using Fe(III)-SMW, the hydroxyl ions were released during the uptake of phosphate. When phosphate was taken up by Fe(III)-SMW, hydroxyl ions were released The phosphate concentration after adsorption significantly decreased as the solid-liquid ratio increased, achieving 100 % uptake when using Fe(III)-SMW (Peleka & Deliyanni, 2009).

According to Ramola *et al*., (2021), at the optimized pyrolysis conditions for the preparation of BRH-C: a pyrolysis temperature of 700 °C, pyrolysis time of 2.3 h, and rice husk–calcite (RH-C) ratio of 4.2:1 (w/w), the maximum removal and adsorption capacities of optimized BRH-C were found to be 87.3 % and 1.76 mg/g, respectively, at low phosphate concentrations. The maximum phosphate removal (54.2 %) and adsorption capacity (10.72 mg/g) were achieved at phosphate concentration of 95 mg/L, 0.24 g of BRH-C, pH 5.4, and contact time of 11.75 h. Phosphate removal by BRH-C was maximum at lower concentrations (10–25 mg/L), whereas phosphate removal by calcite was maximum at higher concentrations (75–125 mg/L)

The study involved pre-treating sugarcane bagasse to remove sugars and greases, followed by carboxymethylation of the fibers, retaining approximately 20 % impurities. Thermal analyses indicated significant changes in carboxymethylated fibers upon addition of Fe^{2+} and PO_4^{3-}. With 4% iron adsorption, carboxymethylated fibers captured

97% of phosphate, compared to 94% on non-carboxymethylated fibers. Adsorption data fitted both Langmuir and Freundlich isotherms, with a maximum adsorption capacity (Q max) of 152 mg/g, surpassing or matching published results. Notably, the process maintained the environmentally safe nature of the starting biomass waste despite minor chemical alterations (Santana *et al*., 2011).

Using *Staphylococcus xylosus* cells treated with Fe(III), phosphate was adsorbed from aqueous solutions. The experimental data was analysed with Freundlich and Langmuir isotherm models. Langmuir isotherm model fit the equilibrium data better than Freundlich isotherm model. At optimal pH 3.0, biomass concentration of 0.5 g/L, and equilibrium period of 60 min, the biosorption capacity of Fe(III)-treated biomass for phosphate was determined to be 70.92 mg/g. 0.14 M HCl effectively desorbate the phosphate from 2.0 g/L of phosphate-loaded biomass (Aryal, 2011).

Using membrane formation and cross-linking, zirconium (IV) loaded cross-linked chitosan (CCP-Zr) was created in this study. It was then examined using FTIR, XRD, SEM, and EDX. Several studies were conducted to investigate the effects of various factors; including the amount of adsorbent used and the initial phosphate concentration of phosphate, the pH level, and co-ion concentration on the phosphate adsorption onto CCP-Zr. Data from experiments were examined using several isotherm and kinetic adsorption models. The Langmuir isotherm model provided the best explanation for the isotherm data with at pH 3 and 303 K, the highest monolayer adsorption capacity is 71.68 mg/g (Xiong *et al*., 2017).

Phosphate was extracted and recovered from waste waters using adsorbents based on metal-loaded agricultural wastes (MLAWs). Agricultural waste-based adsorbents (AWs) for phosphate removal from waste water sources were prepared. In the presence of co-existing ions such as Cl^-, NO_3^-, SO_4^{--}, CO_3^{--}, etc. throughout a broad pH range of 4–9, MLAWs demonstrated excellent phosphate adsorption capability in a short period of time (>1hr). By employing only distilled water, salts, acids, and bases, phosphate-laden adsorbents can be easily restored to up to 80% or more of their original adsorption capacity (Pokhrel *et al*., 2019).

An in-depth characterization of biochar was carried out to study its physical, surface morphological and chemical characteristics using X-ray diffraction, Fourier transform infrared and scanning electron microscopy analyses. The impact of pyrolysis temperatures (300–600 °C) on the biochar yield, the biochar's elemental composition, and its adsorption characteristics was examined. Biochar produced at 600 °C showed a

maximum uptake for both nitrate and phosphate due to its high C content (63.8%), pore volume (0.201 cm^3/g), surface area (204.2 m^2/g) and reduced acidic binding groups. The influence of pH, initial solute concentrations, and contact time on the removal of a single solute at a time by biochar was examined. Results revealed that pinewood-derived biochar had its maximum performance at pH 2, with predicted equilibrium uptakes of 20.5 and 4.20 mg/g for phosphate and nitrate, respectively at initial solute concentrations of 60 mg/L within 360 min (Kuppusamy *et al*., 2021)

Chemically modified sugarcane bagasse was characterized by SEM and FTIR analyses. In batch tests, the phosphate's ability to adsorb from aqueous solutions was studied. The decrease in the value of of $-\Delta G_0$ increasing temperature from 20 °C to 60 °C shows that the sorption process is less favorable at higher temperature. The enhanced amine groups in MSB (modified sugarcane bagasse biochar) were confirmed by the sugar cane's characterization data, and its maximum sorption capacity for phosphate, Q_{max}, was determined to be 1.05 mol g^{-1}. At 2 g L^{-1}, phosphate removal performed at its best of MSB dose and at 20 °C (Bagasse *et al*., 2017).

2.2. Research gap

Diverse strategies for eliminating phosphate (PO_4^{3-}) from water are highlighted by a thorough study of the literature. These strategies range from traditional ones like ion exchange and precipitation to more sophisticated ones like membrane processes. Conventional approaches present obstacles like high operational costs and poor selectivity for target ions. These modified biosorbents offer a promising and economical alternative that may effectively remove even trace amounts of contaminants from aqueous solutions by saponifying RWR to create cation and anion exchangers.

CHAPTER-3

MATERIALS AND METHODS

3.1. Chemical reagents

The chemicals employed were of laboratory grades and their specifications are outlined in the subsequent table.

Table 1: List of chemicals used

Name of Chemicals	Manufacturer Name	% Purity
Sodium Bicarbonate ($NaHCO_3$)	Qualigens fine chemicals	99.9
Ammonium heptamolybdate $[(NH_4)_6MO_7O_{24}.4H_2O]$	Qualigens fine chemicals	98
Potassium Antimony Tartarate $[K(SbO)C_4H_4O_6.1/2H_2O]$	Merck	99
Calcium Hydroxide $[Ca(OH)_2]$	E. Merck	96
Hydrochloric Acid (HCl)	Qualigens fine chemicals	97
Oxalic Acid ($C_2H_2O_4$)	Qualigens fine chemicals	99.5
Sodium Hydroxide (NaOH)	Fischer scientific	98
Ascorbic Acid ($C_6H_8O_6$)	Roche	90
Potassium Dihydrogen Phosphate ($K_2H_2PO_4$)	Qualigens fine chemicals	99
Sodium Chloride (NaCl)	Thermo Fischer scientific	99.5
Sulphuric Acid (H_2SO_4)	Qualigens fine chemicals	98
Sodium Carbonate Na_2CO_3)	Qualigens fine chemicals	98
Aluminium Nitrate	Qualigens fine chemicals	98

3.2. Instruments

The tools utilized for the research are listed below.

Table 2: List of instruments

Instrument name	Model number	Manufacturer	Manufacturing country
Laboratory mill	LM-05	Chinetti	Italy
Sieve	E11	Retsch	Germany
Weighing balance	ASN-224	Phoenix instrument	Germany
Shaker	SF1	Stuart Scientific	United Kingdom
Oven	UN30	Elite Oven	United Kingdom
Digital pH meter	LT-11	Labtronics	India
Spectrophotometer	LT-2802	Labtronics	India
FTIR	10.6.2	PerkinElmer	New Zealand

3.3. Organization of the study

The organization of a study typically followed a structured format that includes:

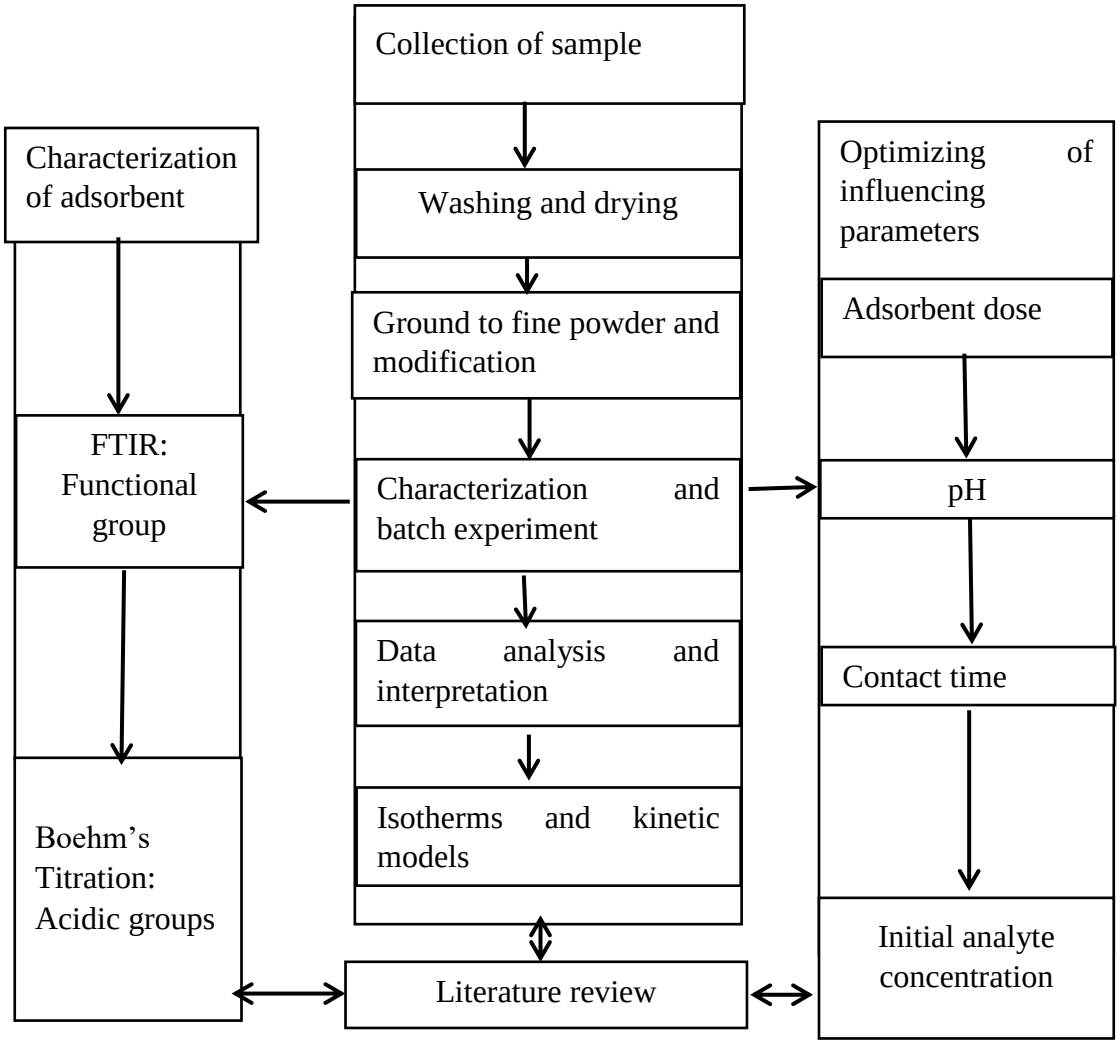

Figure 3: Methodological framework of the study

3.4. Methodological study

The best approach and material for wastewater treatment must be chosen based on the chemistry of the wastewater as well as other criteria including efficiency and quality standards as well as the associated cost.

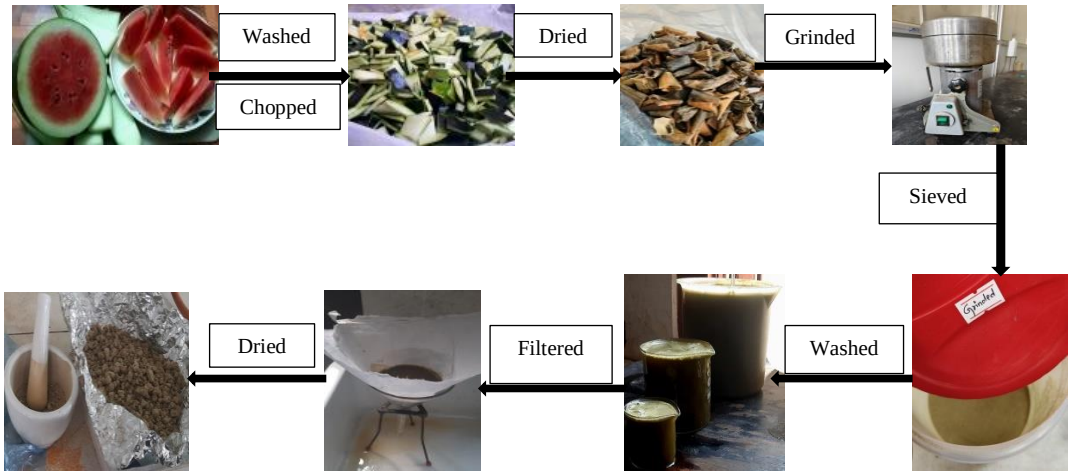

Figure 4: Working process for the preparation of RWR

The laboratory protocols used in the Chemistry Department at the Amrit Campus are described in the above figure. Watermelon rind were first gathered from the market around the New Road, then washed, chopped into small pieces and dried. After being allowed to air dry for ten days, the rind was pulverized into a fine powder known as raw watermelon rind (RWR). The RWR was sieved, cleaned with distilled water, left sun dry for three days and for twenty-four hours in an oven at temperature 65 °C. After that, RWR was treated with $Ca(OH)_2$ and 2 pellets of NaOH to saponify watermelon rind and the product was called saponified watermelon rind (SWR). SWR was then subjected to Al(III) loading Al(III)-loaded SWR was obtained by filtering, drying, and washing the resultant product until it became neutral (Aryal *et al*., 2021).

3.5.Preparation of reagents

3.5.1. Preparation of 1000 mg/L stock phosphate solution

The solution of potassium dihydrogen orthophosphate (KH_2PO_4) was prepared by dissolving 1.432 g of (KH_2PO_4) in a small amount of deionised water. The solution was subsequently transferred into a 1000 mL volumetric flask and filled up to the mark with distilled water after thorough mixing.

3.5.2. Preparation of 5 N sulphuric acid solution

In a 500 mL volumetric flask, 68.8 mL of concentrated sulfuric acid solution (98%) was poured and the solution was mixed and the volume was filled upto mark.

3.5.3. Preparation of ammonium molybdate solution

In 500 mL of volumetric flask 20 g of $(NH_4)_6Mo_7O_{24}\cdot 4H_2O$ was dissolved in distilled water and the volume was filled upto the mark.

3.5.4. Preparation of potassium antimonyl tartarate solution

1.371 grams of $K(SbO)C_4H_4O_6 \cdot 1/2H_2O$ were dissolved in distilled water in a 500 mL volumetric flask and then diluted to volume. It was then stored in the volumetric flask.

3.5.5. Preparation of ascorbic acid solution

By dissolving 1.76 g of compound the solution of 0.1 M ascorbic acid was prepared in small volume of water. After completion of the dissolution, the water was filled up to the mark.

3.5.6. Preparation of combined solution

The different reagents were combined in the following proportions to yield 100 mL of the combined reagent: 50 mL of 5 N H_2SO_4, 5 mL of potassium antimony tartrate solution, 15 mL of ammonium molybdate solution, and 30 mL of ascorbic acid solution. All reagents were mixed at room temperature and were combined in the given ratio. In case of turbidity in the combined reagent, it was gently shaken and allowed to settle until clarity was restored before further steps were taken. The stability of the reagent was maintained by using acetone since the prepared solution was persisted only up to 4 hours.

3.5.7. Preparation of aluminium nitrate solution

The aluminium nitrate solution was prepared in a 250 mL volumetric water dissolving 3.47 g of $Al(NO_3)_3$ in distilled water. After the dissolution the water was filled up to mark.

3.5.8. Preparation of 1.0 M sodium chloride (NaCl) solution

To prepare 1.0 M NaCl solution, 5.8 g of NaCl crystal were dissolved in distilled water in a 100mL volumetric flask. When the solution was ready, it was serial diluted to 0.1 M, 0.05 M and 0.01 M solution for the further experiments

3.5.9. Preparation of 1 M oxalic acid solution

In a 100 mL volumetric flask, 6.3 g of oxalic acid crystal was dissolved and the volume was made up to mark.

3.5.10. Preparation of sodium hydroxide solution

The 5 M NaOH solution was prepared by dissolving 20 g of NaOH pellets were weighed and dissolved in 100 mL of distilled water. After examining with primary standard solution $C_2H_2O_4$, to make Other concentrations of NaOH solutions having strength 1.0 M, 0.5 M, 0.1 M, 0.05 M, 0.01 M were prepared from 5 M NaOH solution were prepared by serial dilution**.**

3.5.11. Preparation of sodium bicarbonate solution

In a 100 mL volumetric flask, 8.4 g of $NaHCO_3$ was first dissolved and the volume was filled up to the mark. Subsequently, the solution was diluted to generate 0.1 M, 0.05 M, and 0.01 M solutions for the additional experiments.

3.5.12. Preparation of sodium carbonate solution

The concentration of 1 M sodium carbonate solution was prepared by dissolving in 100 mL volumetric flask. After the dissolution, 0.01 M, 0.05 M, and 0.1 M solutions were prepared by the serial dilution.

3.5.13. Preparation of calcium hydroxide solution

12.5 g of $Ca(OH)_2$ was dissolved in 500 mL of distilled water and then the volume was filled up to mark.

3.6. Preparation of Al(III)-loaded saponified watermelon rind

3.6.1. Collection and pre-treatment of raw watermelon rind

First of all, watermelon rind was collected from local fruit shops at New Road and Ratnapark, Kathmandu. They were chopped and washed many times with deionized water. The pieces cut to smaller ones, so as to ensure complete drying then left to dry in the sun for about five days. Small pieces of dried watermelon rind were also dried into oven for 24 hrs. at 60 °C. Then the dried pieces were grinded in the laboratory mill followed by sieving using 250 micron sieve. Then the powder form sample was washed with distilled water and again dried. A sum of 250.9 g of dried fine powder was obtained finally, referred as raw watermelon rind, abbreviated as RWR.

3.6.2. Saponification of RWR

500 ml saturated solution of $Ca(OH)_2$ was first prepared in distilled water. 100 grams of RWR was then accurately weighed out and treated with $Ca(OH)_2$ solution adding 2 pellets of NaOH. It was then shaken in a mechanical shaker for 24 hours under room temperature condition with a speed of 220 rpm. The wet product obtained after this treatment process was then rinsed repeatedly with distilled water, following decantation process till neutrality (pH-7). It was then dried at 60 degree Celsius in hot air oven for 24 hours. 90 grams of dried powder was ultimately obtained. That powder was termed as saponified watermelon rind, abbreviated as SWR.

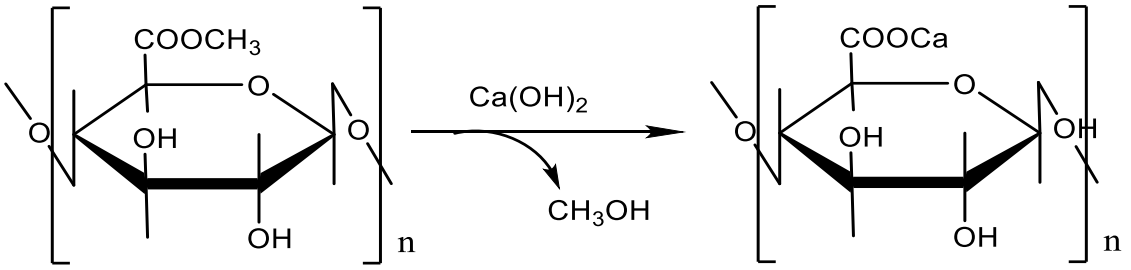

Methyl ester in RWR SWR

Scheme 2: Reaction of SWR formation

3.6.3. Preparation of Al(III)-loaded saponified watermelon rind (Al-SWR)

10 grams of SWR were mixed with 250 mL of 1.5 M Al(III) salt solution at pH 2 to 4. Then the mixture was shaken for 24 hours at room temperature. It was filtered and washed until reaching a pH of 7. Then the residue was dried at temperature 65 °C resulting the final product called as Al(III)-SWR.

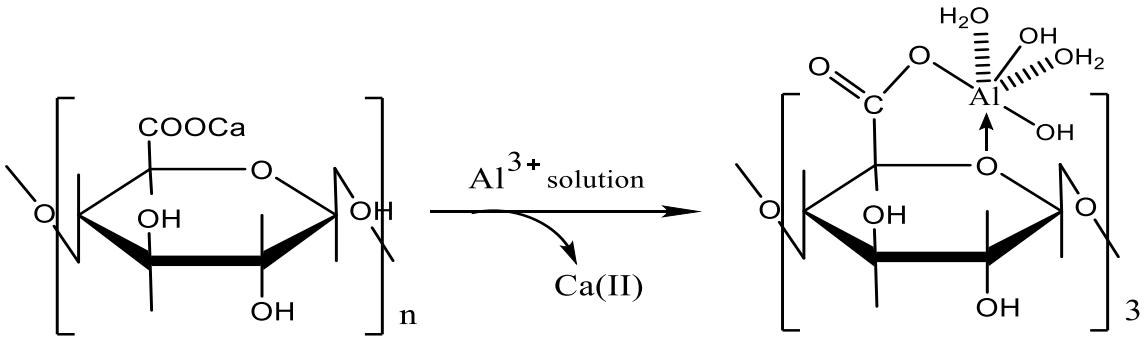

SWR Al-SWR

Scheme 3: Reaction for preparation of Al-SWR

3.6.4. Adsorption of phosphate anion by Al(III)-SWR

1 gram of Al(III)-SWR was combined with 100 mL of 2 M phosphate solution. The mixture was shaken for 24 hours at room temperature. It was filtered and washed until reaching a pH of 7 then dried in an oven for 24 hrs. at temperature 65 °C. The obtained product is termed as Al(III)-SWR@PO4.

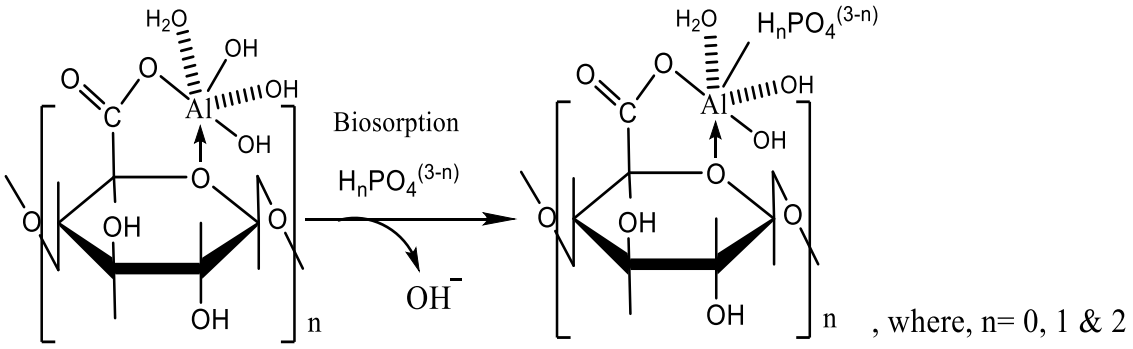

Scheme 4: Adsorption mechanism of phosphate

3.6.5. Preparation of calibration curve for spectrophotometric determination of PO_4^{3-}

For the calibration curve, solutions containing different concentrations of phosphate (PO_4^{3-}) ranging from 0.5 to 10 mg/L were accurately prepared through sequential dilution from a stock solution. The absorbance of each solution was measured using a spectrophotometer at the wavelength of maximum absorbance (λ_{max}), which was determined to be 765 nm. A graph plotting absorbance against phosphate concentration was generated. The slope of the resulting straight line was calculated, and this value was utilized to determine the unknown concentration of phosphate in the solution.

3.6.6. Determination of point of zero charge (pHpzc)

Point of zero charge analysis is crucial for assessing the surface charge of the biosorbent. It indicates that surface charge of Al(III)-SWR is pH-dependent. The pH level of suspension medium, denoted as the point of zero charge (pHpzc), holds significance in comprehending adsorption mechanisms. Below the pHpzc, particle surfaces carry a positive charge, facilitating the adsorption of anions. Conversely, above the pHpzc, surfaces develop a negative charge, thus promoting the adsorption of cations.

To investigate pHpzc, solutions of 0.01 M, 0.05 M, and 0.1 M NaCl were prepared in 50 mL volumetric flasks. Subsequently, 50 mg of Al(III)-SWR was mixed with 10 mL of 0.01 M NaCl, and the mixture was shaken for 24 hours at varying pH levels ranging from 1 to 12. The initial and final pH values were recorded. This experimental procedure was repeated for the 0.05 M and 0.1 M NaCl solutions. By plotting the change in pH (ΔpH) against the initial pH for all three NaCl solutions, the pHpzc was determined as the point where the pH change equals zero.

3.7. Characterization Techniques

3.7.1. Boehm's titration

0.5 grams of RWR and Al-SWR were shaken individually with 50 mL of solutions containing 0.1 M HCl, 0.1 M NaOH, 0.1 M Na_2CO_3, and 0.15 M $NaHCO_3$ for 24 hours. The resulting mixtures were then filtered, and the filtrate was collected for titration. Subsequently, 10 mL of the filtrate was treated with either 0.1 M HCl or 0.1 M NaOH, and the amounts consumed in each case were calculated in mol/g. Changes in functional group content resulting from the modification were analyzed. Based on Boehm, that NaOH neutralizes carboxylic, lactonic, and phenolic groups, Na_2CO_3 neutralizes both carboxylic and lactonic groups, and $NaHCO_3$ neutralizes carboxylic groups, the amount of acidic groups on the adsorbent was determined. The quantity of HCl that interacted with the adsorbent allowed for the calculation of the number of surface basic sites.

3.7.2. Fourier transform infrared (FTIR) spectroscopy

Fourier-transform infrared (FTIR) spectroscopy serves as a versatile analytical method utilized to characterize functional groups and molecular configurations across diverse substances by analyzing their infrared absorption spectra. FTIR spectroscopy functions by detecting how molecules absorb particular frequencies of infrared radiation resulting in characteristic absorption peaks that correspond to different molecular vibrations. By irradiating a sample with infrared light and measuring the intensity of transmitted or absorbed light at different wavelengths, FTIR spectroscopy provides valuable information about the chemical composition and structure of a material. This technique finds widespread applications in fields such as chemistry, pharmaceuticals, polymers, and materials science for qualitative and quantitative analysis, as well as for monitoring chemical reactions and identifying unknown compounds.

3.8. Batch adsorption studies

Batch adsorption studies were performed by preparing a phosphate solution. The strength of phosphate solution was determined by using calibration curve which was found to be 9.96 mg/L (≈10 mg/L). Several batch studies were done as follows:

3.8.1. Effect of pH

Firstly, 10 mg of adsorbent were taken in 12 conical flasks. Then 10 mL of phosphate solutions of pH 1.3-11.8 were prepared by using 0.01 M NaOH and 0.01 M HCl solutions. 5.0 mL of the prepared solutions were poured into the conical flasks and left

were kept to determine the initial concentrations of the phosphate solutions. Thus prepared solutions were shaken in a rotatory flask shaker for 24 hrs. at 220 rpm. Then the initial concentrations of the solutions were determined by using combined solutions and spectrophotometer. After shaking for 24 hrs., final concentration of each solution was determined using spectrophotometer. The optimum pH at which the maximum adsorption occurred were determined for both RWR and Al(III)-SWR.

3.8.2. Effect of adsorbent dosages

Different masses of Al(III)-SWR, 1 g/L, 2 g/L, 4 g/L, 6g/L, 8 g/L, 10 g/L, 12 g/L, 14 g/L, 16 g/L, 18g/L and 20 g/L were taken in 11 conical flasks and 5 mL of 10 mg/L of solution was added to each of the conical flask. The mixture was shaken in rotatory flask for 24 hrs. in 220 rpm and the amount of phosphate adsorbed at different amount of adsorbent dosages were calculated in mg/L.

3.9. Adsorption kinetic studies

Based on the data obtained from pH studies, the adsorption capacity of raw watermelon rind (RWR) was minimal. Consequently, only the Al(III)-loaded watermelon rind (Al(III)-SWR) was utilized for the kinetic studies of the adsorbent. For the kinetic studies, a solution with a concentration of 10 mg/L was used. In this experiment, 10 mg of the adsorbent were placed into each of 18 conical flasks, and 10 mL of phosphate solution was added to each flask. Following the addition of the solution, the samples were immediately subjected to shaking. The amount of phosphate adsorbed was measured at intervals of 5, 10, 15, 30, 45, 60, 90, 120, 150, 180, 240, 300, 360, 420, 480, 540 minutes and 24 hrs. The final concentration of each time was determined by using UV-spectrophotometer.

3.10. Adsorption isotherm studies

The effect of initial phosphate concentration on adsorption was studied by preparing solutions with varying phosphate concentrations. Solutions were prepared with phosphate concentrations of 10.20 mg/L, 24.40 mg/L, 52.0 mg/L, 103.07 mg/L, 147.70 mg/L, 207.40 mg/L, 258.0 mg/L, 308.25 mg/L, 408.0 mg/L, 493.89 mg/L, and 596.50 mg/L. For the adsorption experiments, 5 mL of each solution was placed into separate conical flasks, each containing 10 mg of the adsorbent. Then the solutions were shaken for 24 hrs. in the rotatory flask and final concentrations of each solution were determined by using UV-spectrophotometer.

CHAPTER-4

RESULTS AND DISCUSSION

4.1. Watermelon rind and its chemical modification

Pectin is weakly acidic polysaccharides consists of pectic acid containing methyl esterified carboxylic acid functional groups. Treatment with $Ca(OH)_2$ causes the hydrolysis of these methyl esters, converting them into pectic acid salts. Acting as materials for weakly acidic cation exchange, the resulting calcium salt of pectic acid lays the foundation for saponified watermelon (SWR). SWR is furnished with exchangeable Ca(II) ions, which can be interchanged with cations. To promote the creation of anion exchange sites, modification of SWR is mandatory.

4.2. Characterization of biosorbent

4.2.1. FTIR analysis

The FTIR analysis was performed to identify the functional groups present on the surfaces of RWR, SWR, Al(III)-SWR and Al(III)-SWR@PO_4^{3-} within the spectral range of 4000 to 400 cm^{-1}. The peak observed in RWR at 3347 cm^{-1} corresponds to stretching vibration of OH-bond of methoxyl group in pectin and lignin on the surface of RWR. The peak at 2879 cm^{-1} is due to the stretching vibration of C-H and -CH_2 bonds whereas 1375 cm^{-1} and 813 cm^{-1} indicate the bending vibration of C-H bonds. A characteristic stretching peak of carboxyl group is observed at 1741 cm^{-1} in RWR is of C=O and –COO groups. After $Ca(OH)_2$ treatment, the peak observed around 1741 cm^{-1} disappeared and new peak observed around 1612 cm^{-1} indicating the presence of O-Ca bond of calcium pectate salt. Also, peaks appeared in SWR sample at 3421 cm^{-1} is less intense than that of RWR indicating free hydroxyl group ,1183 cm^{-1} and 1011 cm^{-1} are due to the stretching vibrations of C=O bonds in ethers and C-O bonds in alcohols, respectively. After Al(III)-loading the peak changed to lower frequency due to the replacement of Ca(II) by Al(III) of greater atomic mass. The peaks 3327 $cm^{-1,}$ 2356 cm^{-1}, and 1055 cm^{-1} indicate the stretching vibration of O-H bond, C≡C bond of alkyne, C-O bond of the ester and C-O bonds of alcohol, also a peak 1282 cm^{-1} was appeared because of stretching vibration. Similarly, stretching vibrations of O-H bonds in phenol, C-H bonds in alkane, C=C bonds in alkene and C-O bonds in esters show the peaks at 3303 cm^{-1}, 2973 cm^{-1}, 1532 cm^{-1} and 1316 cm^{-1}. The infrared peak indicates either the bending vibration of the C-H bond or the stretching vibration of the C-O bond shows IR peak at 1016 cm^{-1}. This results show that

the intensity and position of the peaks change across each sample indicating alteration in the chemical environment. The broad O-H peaks in each sample shift slightly in wavenumber showing difference in H-bonding interaction.

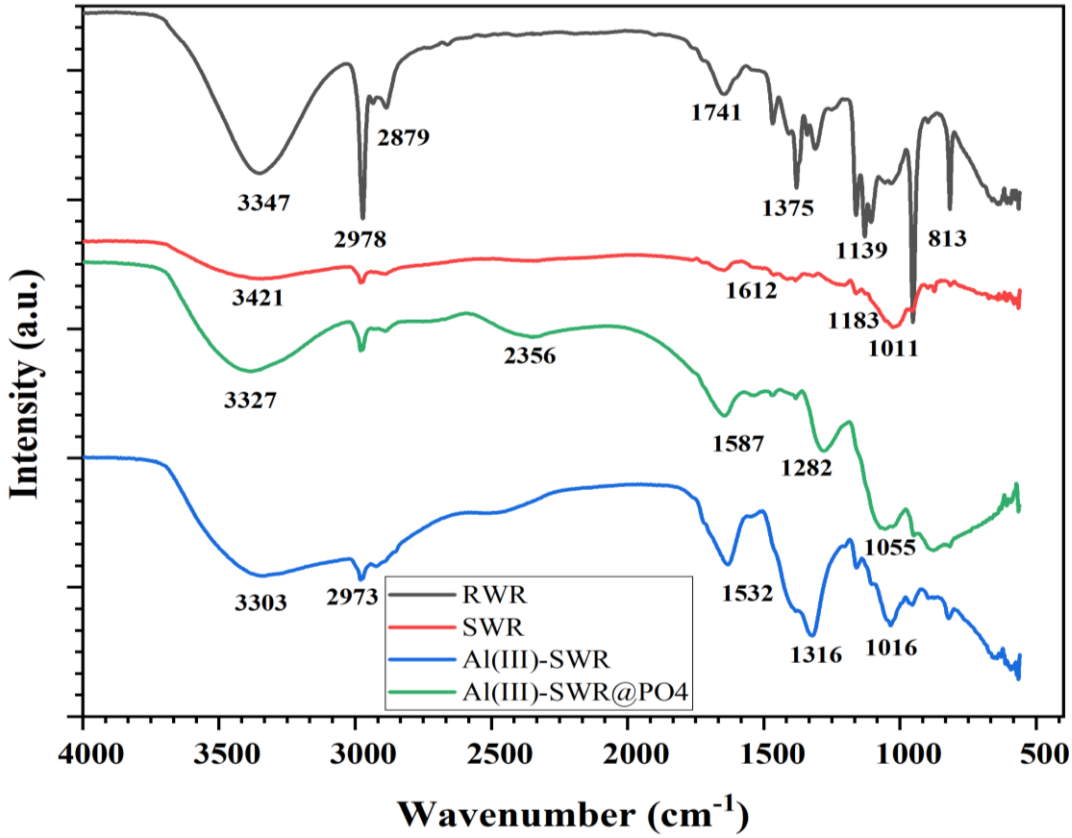

Figure 5: FTIR spectra of RWR, SWR, Al (III)-SWR and Al(III)-SWR@PO_4^{3-} (400-4000 cm^{-1})

4.2.2. Point of zero charge (pHpzc) determination

The pH of solution in relation to pHpzc of adsorbent affects phosphate adsorption onto Al(III)-SWR adsorbent. The adsorbent's surface charge and the electrostatic interactions of the adsorbent with phosphate ions at different pH levels affect the effectiveness of phosphate adsorption. The curves for different NaCl concentrations (0.1 M, 0.05 M, and 0.01 M) were observed. Higher ionic strength (0.1 M) was found to show a slightly higher change in pH (ΔpH) at high initial pH values compared to 0.05 M and 0.01 M NaCl solutions. This was because higher ionic strength screens surface charges more effectively, reducing electrostatic interactions. The pHpzc of Al(III)-SWR was found to be 4.0. This means that below pH 4.0, the surface is positively charged, enhancing adsorption through electrostatic attraction to negatively charged phosphate ions, at pH 4.0, the surface charge is neutral, resulting in moderate adsorption driven by specific chemical interactions and above pH 4.0, the surface becomes negatively charged, leading

to decreased adsorption due to electrostatic repulsion. Thus, optimal phosphate adsorption occurs in acidic conditions below the pHpzc.

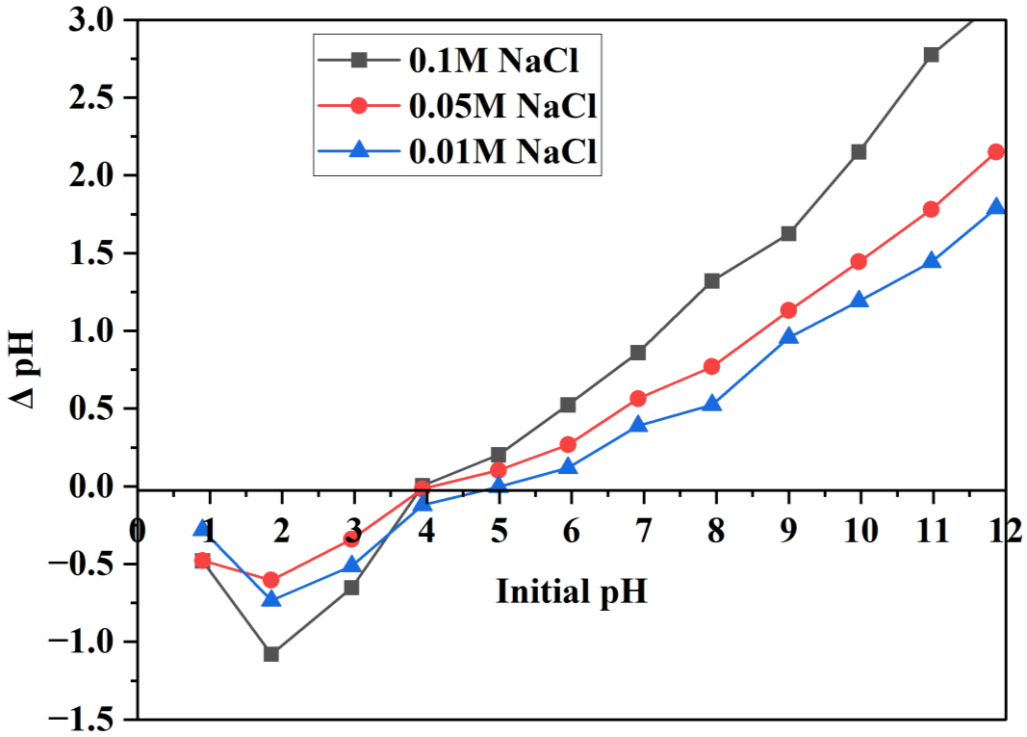

Figure 6: Point of zero charge of Al(III)-SWR at different pH

4.2.3. Boehm's titration

The adsorbent, RWR and Al(III)-SWR were treated with 0.05M HCl, 0.05 M NaOH, 0.05 M Na_2CO_3 and 0.05 M $NaHCO_3$ solutions. The results obtained from the titrations followed by calculations are as given in the following table:

Table 3: Concentration of surface functional groups

Sample	Carboxylic group (mol/kg)	Lactonic group (mol/kg)	Phenolic group (mol/kg)
RWR	1.50	1.02	1.13
Al(III)-SWR	1.61	1.07	1.38

According to the Boehm's titration, the concentrations of surface functional groups on Al(III)-SWR is slightly higher than in RWR. The RWR was found to contain 1.50 mol/kg carboxylic groups, 1.02 mol/kg of lactonic group and 1.13 mol/kg of phenolic group. Similarly, 1.61 mol/kg, 1.07 mol/kg and 1.38 mol/kg of carboxylic, phenolic and lactonic groups were found to be present in the Al(III)-SWR sample. Due to this higher

concentration of carboxylic, phenolic and lactonic groups in Al-SWR, the adsorption occurred more effectively because of the presence of more active sites for adsorption.

4.3. Determination of λ_{max} & Construction of calibration curve

A calibration curve is a graphical representation of the relationship between the concentration of phosphate and the absorbance or fluorescence intensity. It's a basic method in analytical chemistry employed to measure the concentration of unknown samples by comparing with standard samples. For the construction of calibration curve, maximum wavelength (λ_{max}) should be determined. The maximum absorption wavelength (λ_{max}) was calculated by plotting absorbance against wavelength as follows.

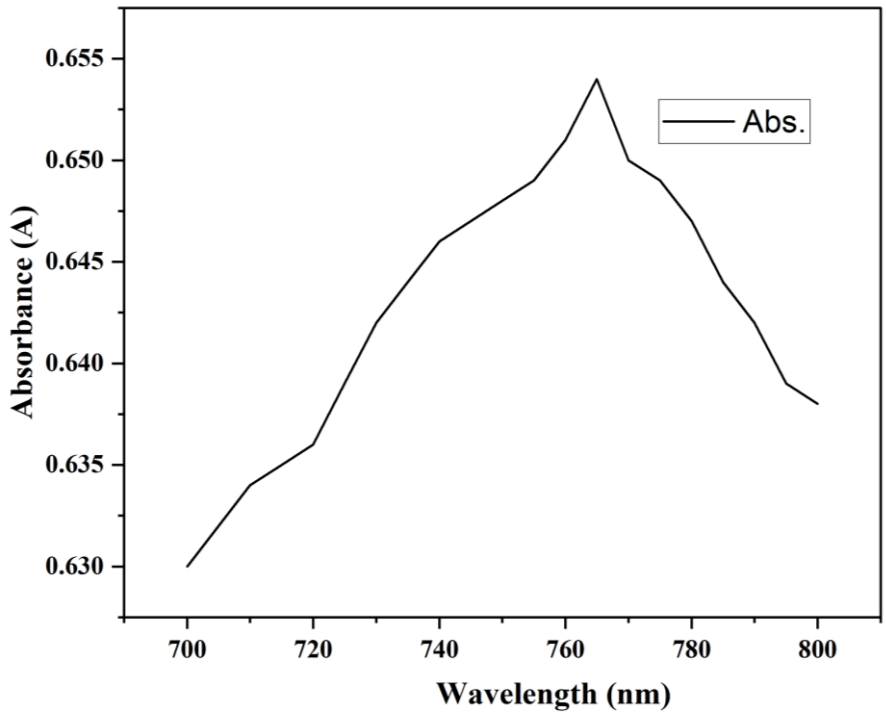

Figure 7: Maximum wavelength (λ_{max}) curve of phosphate solution

The absorbance of unknown solutions was derived by establishing its maximum wavelength using a 0.5 parts per million (ppm) phosphate solution, which revealed a maximum wavelength (λ_{max}) of 765 nanometers (nm) (Zhang *et al*., 2011). Subsequently, phosphate solutions with concentrations ranging from 1 to 10 ppm were prepared, and their absorbance was measured at a consistent λ_{max}. The slope derived from the graph plotting concentration against absorbance was utilized to determine the strength of the unknown solution. The concentration of the unknown solution was determined by dividing the slope with absorbance. After the calculation, the concentration of unknown solution was found to be 9.961 ppm (≈ 10 ppm).

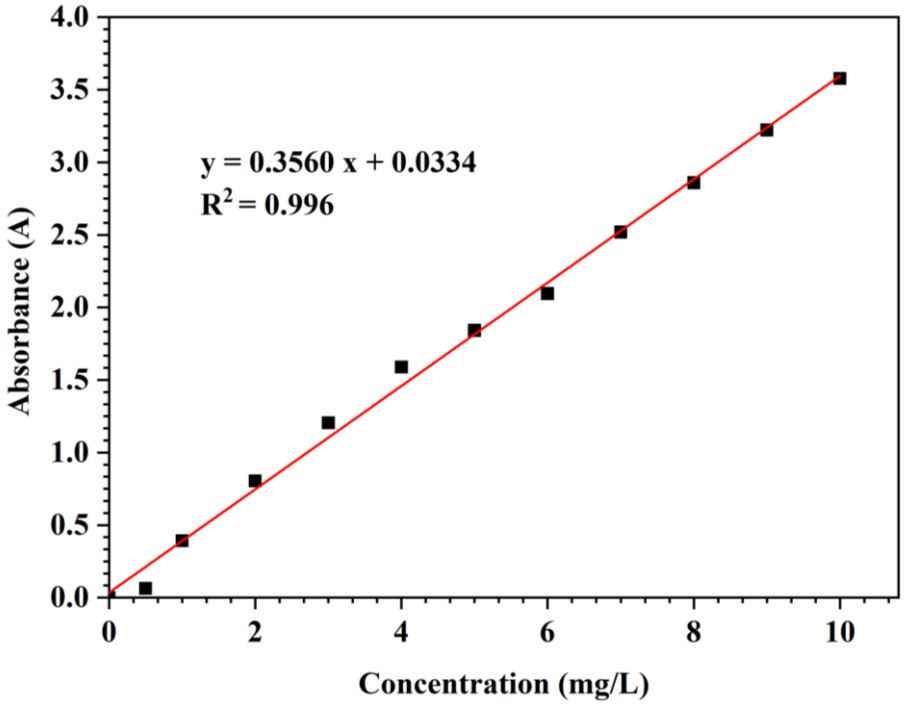

Figure 8: Concentration vs. Absorbance plot of the phosphate solution

4.4. Batch studies

4.4.1. Effect of pH

Phosphate ion adsorption depends on the distribution of phosphate species in the solution as well as the surface properties of the adsorbent. Higher phosphate adsorption efficiency was demonstrated by Al(III)-loaded saponified watermelon rind as adsorbent. Phosphate sequestration increased progressively from 18.25% at pH 1.78 to a maximum of 87.91% at pH 3.90, and then it fell gradually after pH 5.0, suggesting that pH 3.90 is the ideal pH. Since, around pH 2-7, $H_2PO_4^-$ becomes the dominant species reaching almost 100 % around pH 4, adsorption of dihydrogen phosphate occurred during the process. The pHpzc of the adsorbent was determined to be 4.0, indicating that the Al(III)-SWR surface is positively charged at pH values below 4.0, which promotes phosphate anion adsorption through Coulombic interaction. On the other hand, the surface becomes negatively charged and inhibits phosphate anion adsorption at pH values greater than pHpzc. The hydroxyl ligand in the coordination spheres of Al(III)-SWR easily exchanged with phosphate anion through the ligand exchange mechanism.

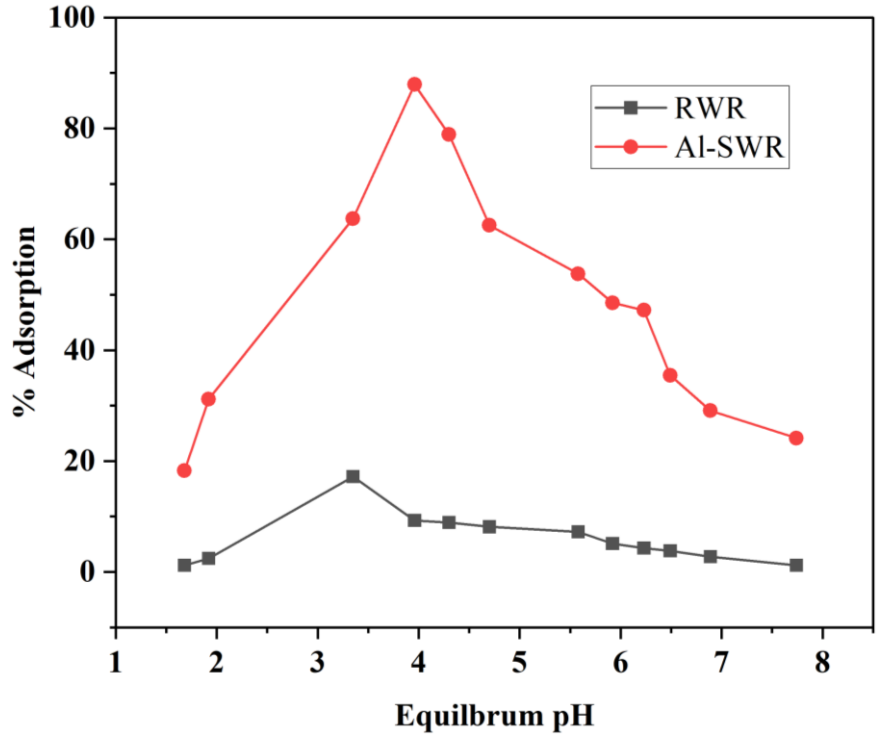

Figure 9: Plot of Equilibrium pH vs. % Adsorption of the phosphate solution

4.4.2. Effect of adsorbent dosages

The adsorption of phosphate is directly influenced by the amount of adsorbent used. The effectiveness and capacity of phosphate removal can be significantly altered by altering the dosages. It was observed that as the dosage of the adsorbent increased, so did the adsorption. At the beginning (0-5 g/L), a sharp decrease in the equilibrium concentration was observed. This indicated that increasing the adsorbent dosage significantly reduced the adsorbate concentration in the solution suggesting the high adsorption efficiency at low dosages. From 5 g/L to 15 g/L, the decrease in the equilibrium concentration continued but at a slower rate indicating the saturation of adsorption sites. Beyond 15 g/L, the equilibrium concentration stabilized and remained constant, even with further increased in adsorbent dosages indicating that adsorption sites are fully occupied.

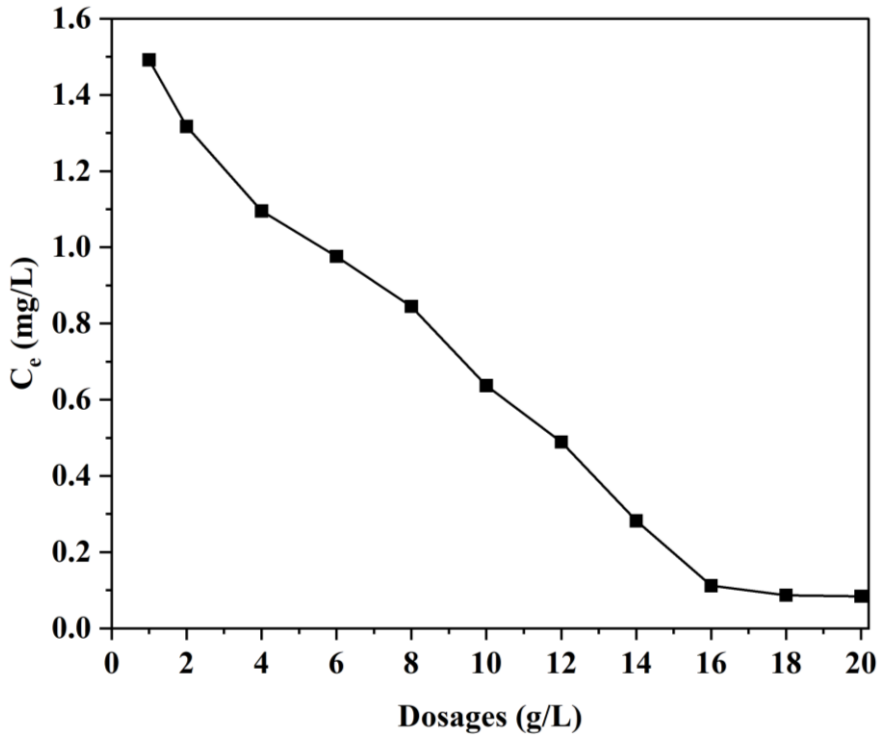

Figure 10: A plot of doses of Al(III)-SWR vs. equilibrium concentration of phosphate solution

4.4.3. Effect of contact time

The adsorption of phosphate by raw watermelon rind (RWR) was insignificant across the entire pH range tested. Kinetic studies of Al(III)-loaded saponified watermelon rind (SWR) at pH 4.05 shown in **Figure 11(a)** had indicated a progressive increase in phosphate adsorption with contact time initially, followed by a slowing down and eventual plateau at 360 min. From the value of coefficient of determination, the adsorption of phosphate was found to be well described by pseudo second order kinetic model.

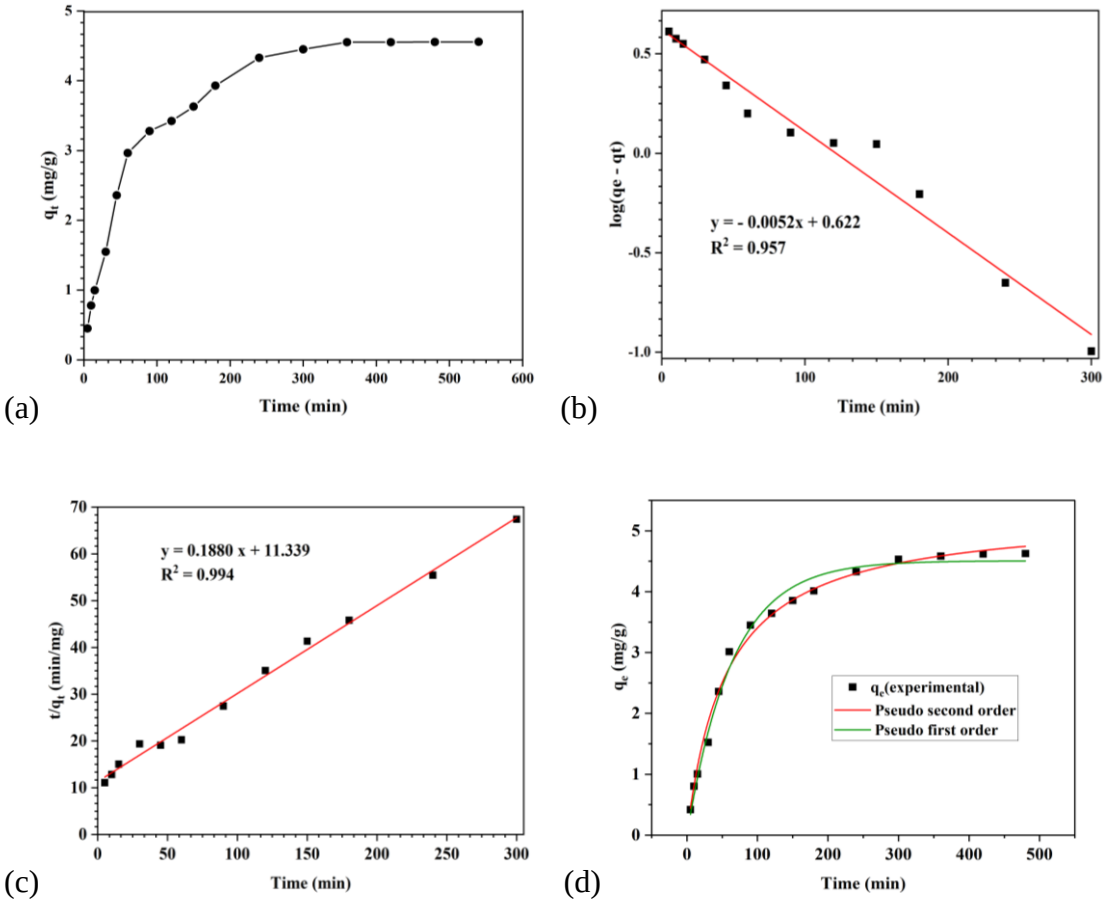

Figure 11: Adsorption of phosphate onto Al(III)-SWR (a) Influence of contact time (b) Plot of pseudo-first-order (c) Plot of pseudo-second-order and (d) Non-linear kinetics of phosphate adsorption onto Al(III)-SWR

Table 4: Kinetic parameters for the adsorption of phosphate onto Al(III)-SWR

Kinetic models	Parameters	Values
Pseudo-first-order	K_1 x 10^{-4} (min^{-1})	1.561
	q_e, exp. (mg/g)	4.507
	R^2	0.989
Pseudo-second-order	K_2 x 10^{-3} (g/mg min)	3.403
	q_e, exp. (mg/g)	5.2948
	R^2	0.9915

Table 4 represented the kinetic parameters for the adsorption of phosphate onto Al(III)-SWR. The table compares the parameter for two pseudo first order and pseudo second order kinetic models and values of R^2 suggested that, the adsorption isotherm followed pseudo second order model.

4.4.4. Effect of initial concentration

The initial concentration of an anion typically increased its adsorption onto a surface until a saturation point is reached. The adsorption isotherm represents the relationship between the amounts of adsorbate adsorbed onto investigated adsorbent with the residual concentration of phosphate. Figure showed the adsorption isotherm of phosphate using Al(III)-SWR. As shown in **Fig. 12(a)** the phosphate adsorption onto Al(III)-SWR increased at lower concentration whereas it was found to attain constant value at higher concentration. The experimental data were modeled using Langmuir isotherm **Fig. 12(b)** and Freundlich isotherms **Fig. 12(c). Fig. 12(d)** which showed that the experimental data was in accordance with the Langmuir isotherm model.

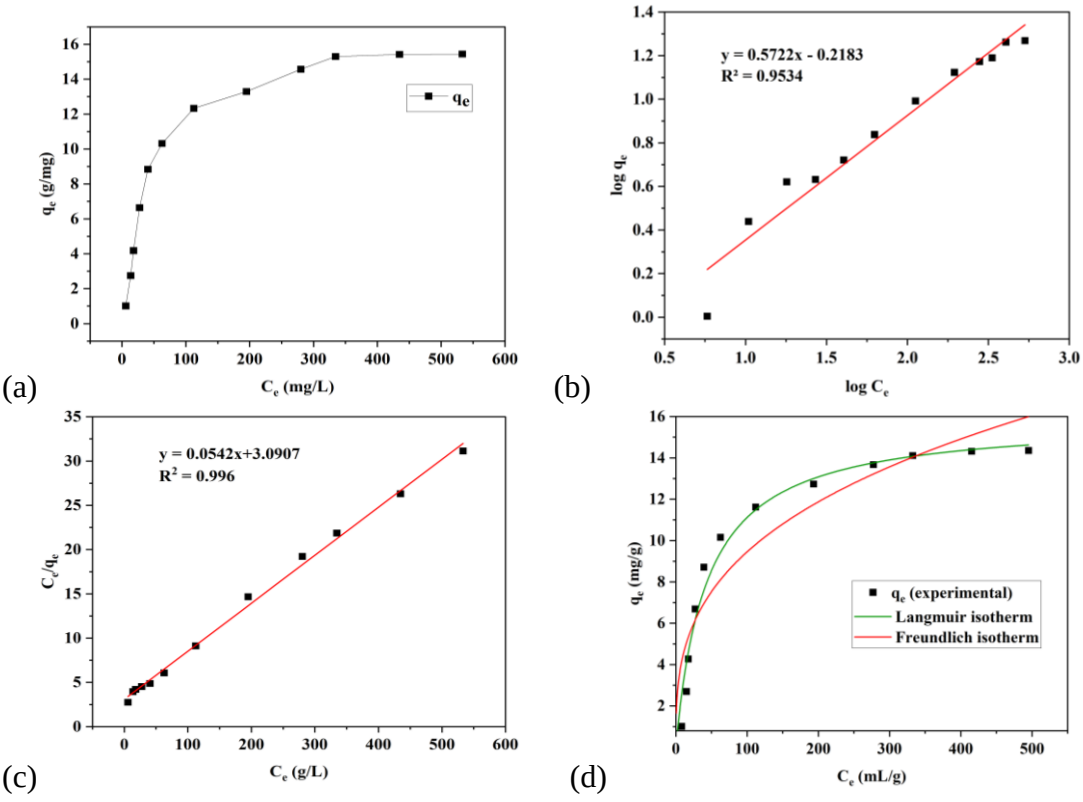

Figure 12: Adsorption of phosphate on to Al(III)-SWR (a) Influence of initial concentration (b) Freundlich isotherm (c) Langmuir isotherm, and (d) non-linear isotherm for the adsorption of phosphate onto AL(III)SWR

Table 5: Isotherm parameters for the adsorption of phosphate onto Al(III)-SWR

Models	Parameters	Values
Langmuir	q_{max}, cal. (mg/g)	15.958
	b (L/mg)	0.0232
	R^2	0.978
Freundlich	K_F (mg/g)	2.077
	1/n	0.328
	R^2	0.862

Table 5 represented the isotherm parameters for the adsorption of phosphate onto Al(III)-SWR. The table compares the parameter for two Langmuir and Freundlich isotherm models and values of R^2 suggested that, the adsorption isotherm followed Langmuir isotherm model.

Table 6: Comparison of maximum adsorption capacities of different adsorbents

Adsorbents	q_{max} (g/mg)	References
Powdered activated carbon	3.51	Muhmad *et al*., 2024
Acid-treated polygorskites	6.64	Hengpeng *et al*., 2005
Acid and thermal treated polygorskites	8.31	Hengpeng *et al*., 2005
Zr-loaded watermelon rind	27.63	Biswas *et al*., 2008
Zr-loaded orange gel waste	13.94	Aryal *et al*., 2021
$Mg(OH)_2$ treated bentonides	3.435	Bouraie *et al*., 2017
Fe-loaded activated carbon	2.874	Braun *et al*., 2018
La-loaded pine needles	2.43	Wang *et al*., 2015
Modified almond wooden sheel	14.71	Taraji *et al*., 2020
Al-loadedwatermelon rind	15.95	**This study**

The maximum phosphate adsorption capacity of Al(III)-SWR is made analogous with some other studies to evaluate the potentiality of adsorbent. It was found that, this study demonstrated a notably higher adsorption capacity for phosphate using Al(III)-loaded watermelon rind achieving a maximum adsorption value of 15.95 mg/g.

4.5.Phosphate adsorption mechanism

The bonding between Al(III) and pectic acid involves the interaction of aluminium ions (Al^{3+}) with the carboxyl groups (-COOH) of pectic acid. All the positive charges of loaded Al(III) ions are impossible to be neutralized by Carboxylic groups due to large steric hindrance caused by big polymeric chains of pectic acid. Therefore, only one or two positive charge of the loaded Al(III) ions are neutralized by anionic species such as hydroxyl and carboxyl groups that undergo ligand exchange reaction with phosphate anion during adsorption.

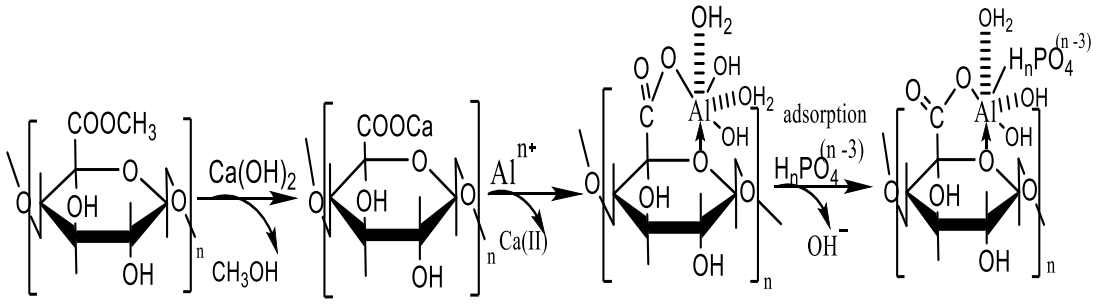

Scheme 5: Adsorption mechanism of phosphate on Al(III)-SWR

Scheme 5 shows the detailed mechanism of phosphate adsorption in Al(III) loaded watermelon rind. Initially, methyl esterified carboxyl group of pectic acid is reacted with calcium hydroxide, then the carboxylate groups of pectic acid are coordinated with calcium ions resulting the formation of calcium pectate salt. When the Al(III) ions are introduced, calcium ions are replaced because of high affinity of Al(III) ions, forming aluminium carboxylate complex. The complex undergoes ligand exchange mechanism where (-OH) group of aluminium carboxylate complex is replaced by $H_nPO_4^{(n-3)}$ (n= 1 or 2) present in the aqueous solution.

CHAPTER-5
CONCLUSIONS AND SUGGESTIONS

5.1. Conclusions

The study used Al-(III)-SWR as the biosorbent to investigate phosphate biosorption from aqueous solutions. Watermelon rind were impregnated with Al(III) and then saponified with $Ca(OH)_2$ to create Al(III)-SWR. The importance of carboxyl functional groups in biosorption was suggested by FTIR analysis. The study also investigated the effects of pH, effect of contact time, effect of adsorbent doses and effect of initial concentration on the biosorption of phosphate. The point of zero charge (pHPZC) of the biosorbent was determined to be 4.0. The highest phosphate loading of Al(III)-SWR calculated using the Langmuir isotherm model was 15.95 mg/g. The Langmuir isotherm model, which depicts the adsorption of phosphate forming a monolayer, provides a better understanding of how phosphate binds to Al(III)-SWR. Kinetic analysis revealed that the PSO kinetic model accurately describes the experimental data. Al(III)-SWR demonstrated superior performance in phosphate adsorption compared to other reported biosorbents. These results highlight Al(III)-SWR as a promising, cost-effective material for removing phosphate from aqueous solution.

5.2.Limitations of the study

a. No additional purification of chemicals were performed before the experiment.
b. The characterizations like SET, EDX, XRD ICP-MS, XPS etc. weren't performed.
c. Desorption studies were not done.
d. Phosphate ion was not removed by 100%.
e. Influence of interfering ion was not studied.
f. Impact of temperature on adsorption was not studied.
g. Adsorption and desorption cycles for phosphate ion were not performed.
h. All the experiments were one in the laboratory condition.

5.3. Suggestion for further works

a. Variation of the adsorption capacity at different temperature can be done.
b. Advanced characterization technologies such as ICP-MS, AAS, SEM, TEM and XPS can be used for further information.
c. For evaluating repeated usage and durability (adsorbent cycle test) can be conducted.

d. A desorption study can be done by using other possible eluents.
e. Column studies for biosorption of phosphate can be performed.

REFERENCES

Aryal, R. L., Bhurtel, K. P., Poudel, B. R., Pokhrel, M. R., Paudyal, H., & Ghimire, K. N. (2022). Sequestration of phosphate from water onto modified watermelon waste loaded with Zr (IV). *Separation Science and Technology*, **57**(1), 70-82.

Bellahsen, N., Kakuk, B., Beszédes, S., Bagi, Z., Halyag, N., Gyulavári, T. & Hodúr, C. (2021). Iron-loaded pomegranate peel as a bio-adsorbent for phosphate removal. Water, 13(19), 2709.Ramola, S., Belwal, T., Li, C. J., Liu, Y. X., Wang, Y. Y., Yang, S. M., & Zhou, C. H. (2021). Preparation and application of novel rice husk biochar–calcite composites for phosphate removal from aqueous medium. *Journal of Cleaner Production*, **299**(13), 126802.

Poudel, B. R., Aryal, R. L., Khadka, L. B., Ghimire, K. N., Paudyal, H., & Pokhrel, M. R. (2020). JNSC. *Journal of Nepal Chemical Society*, **41**(1), 56-63.

Bellahsen, N., Kakuk, B., Beszédes, S., Bagi, Z., Halyag, N., Gyulavári, T., ... & Hodúr, C. (2021). Iron-loaded pomegranate peel as a bio-adsorbent for phosphate removal. *Water*, **13**(19), 2709.

Biswas, B. K., Inoue, K., Ghimire, K. N., Harada, H., Ohto, K., & Kawakita, H. (2008). Removal and recovery of phosphorus from water by means of adsorption onto orange waste gel loaded with zirconium. *Bioresource technology*, **99**(18), 8685-8690.

Yadav, D., Kapur, M., Kumar, P., & Mondal, M. K. (2015). Adsorptive removal of phosphate from aqueous solution using rice husk and fruit juice residue. *Process Safety and Environmental Protection*, **94**, 402-409.

Ismail, Z. Z. (2012). Kinetic study for phosphate removal from water by recycled date-palm wastes as agricultural by-products. *International journal of environmental studies*, **69**(1), 135-149.

Ye, H., Chen, F., Sheng, Y., Sheng, G., & Fu, J. (2006). Adsorption of phosphate from aqueous solution onto modified palygorskites. *Separation and Purification Technology*, **50**(3), 283-290.

Mahmud, F. (2024). Removal of Phosphorous, Copper and Zinc from Stormwater Using Powdered Activated Carbon (Pac) Based Water Treatment Residuals.

Faraji, B., Zarabi, M., & Kolahchi, Z. (2020). Phosphorus removal from aqueous solution using modified walnut and almond wooden shell and recycling as soil amendment. *Environmental Monitoring and Assessment*,**192**(6), 373.

El Bouraie, M., & Masoud, A. A. (2017). Adsorption of phosphate ions from aqueous solution by modified bentonite with magnesium hydroxide Mg $(OH)_2$. *Applied Clay Science*, **140**, 157-164.

Vijayaraghavan, K., & Balasubramanian, R. (2021). Application of pinewood waste-derived biochar for the removal of nitrate and phosphate from single and binary solutions. *Chemosphere*, **278**(14), 130361.

Bashyal, N., Aryal, S., Rai, R., Lohani, P. C., Gautam, S. K., Pokhrel, M. R., & Poudel, B. R. (2023). Effective biosorption of phosphate from water using Fe (III)-loaded pomegranate peel. *Chemical and Biochemical Engineering Quarterly*, **37**(2), 67-77.

Antelo, J., Avena, M., Fiol, S., López, R., & Arce, F. (2005). Effects of pH and ionic strength on the adsorption of phosphate and arsenate at the goethite–water interface. *Journal of colloid and interface science*, **285**(2), 476-486.

Romdhane, M. B., Haddar, A., Ghazala, I., Jeddou, K. B., Helbert, C. B., & Ellouz-Chaabouni, S. (2017). Optimization of polysaccharides extraction from watermelon rinds: Structure, functional and biological activities. *Food Chemistry*, **216,** 355-364.

Ajmal, M., Ali Khan Rao, R., Anwar, S., Ahmad, J., & Ahmad, R. (2003). Adsorption studies on rice husk: Removal and recovery of Cd(II) from wastewater. *Bioresource Technology*, **86**(2), 147–149.

Franco, D., Silva, L. F., da Boit Martinello, K., Diel, J. C., Georgin, J., Netto, M. S., ... & Dotto, G. L. (2021). Transforming agricultural waste into adsorbent: application of Fagopyrum esculentum wheat husks treated with H_2SO_4 to adsorption of the 2, 4-D herbicide. *Journal of Environmental Chemical Engineering*, **9**(6), 106872.

Çelebi, H., Gök, G., & Gök, O. (2020). Adsorption capability of brewed tea waste in waters containing toxic lead (II), cadmium (II), nickel (II), and zinc (II) heavy metal ions. *Scientific reports*, **10**(1), 17570.

Aryee, A. A., Mpatani, F. M., Kani, A. N., Dovi, E., Han, R., Li, Z., & Qu, L. (2021). A review on functionalized adsorbents based on peanut husk for the sequestration of pollutants in wastewater: Modification methods and adsorption study. *Journal of Cleaner Production*, **310**(3)**,** 127502.

M. C., Spessato, L., Silva, T. L., Lopes, G. K., Zanella, H. G., Yokoyama, J. T & Almeida, V. C. (2021). H3PO4–activated carbon fibers of high surface area from banana tree pseudo-stem fibers: adsorption studies of methylene blue dye in batch and fixed bed systems. *Journal of Molecular Liquids*, **324**(4)**,** 114771. 6/S0960-8524(02)00159-1.

Sarkar, S., Tiwari, N., Basu, A., Behera, M., Das, B., Chakrabortty, S., & Tripathy, S. K. (2021). Sorptive removal of malachite green from aqueous solution by magnetite/coir pith supported sodium alginate beads: Kinetics, isotherms, thermodynamics and parametric optimization. *Environmental Technology & Innovation*, **24**(3), 101818.

Ahmadi, A., Prasad, R., Kumar, D., Singh, N., Prasad, V., & Paul, A. (2017). *An economic analysis of production of watermelon in Allahabad District, Uttar Pradesh India*.

Ofomaja, A. E. (2007). Sorption dynamics and isotherm studies of methylene blue uptake on to palm kernel fibre. *Chemical Engineering Journal*, **126**(1), 35-43.

Kaur, R., Singh, J., Khare, R., & Ali, A. (2012). Biosorption the possible alternative to existing conventional technologies for sequestering heavy metal ions from aqueous streams: a review. *Universal Journal of Environmental Research & Technology*, **2**(4).

Amin, M. T., Alazba, A. A., & Manzoor, U. (2014). A review of removal of pollutants from water/wastewater using different types of nanomaterials. *Advances in Materials Science and Engineering*, 2014, 1–24.

Wang, X., Liu, Z., Liu, J., Huo, M., Huo, H., & Yang, W. (2015). Removing phosphorus from aqueous solutions using lanthanum modified pine needles. *PLoS One*, **10**(12), e0142700.

Aryal, M. (2011). Colloids and Surfaces A : Physicochemical and Engineering Aspects Equilibrium , kinetics and thermodynamic studies on phosphate biosorption from aqueous solutions by Fe (III) -treated Staphylococus xylosus biomass: Common ion effect. *Colloids and Surfaces A: Physicochemical and Engineering Aspects*, **387**(1–3), 43–49.

Aryal, M., & Liakopoulou-Kyriakides, M. (2011). Equilibrium, kinetics and thermodynamic studies on phosphate biosorption from aqueous solutions by Fe(III)-treated Staphylococus xylosus biomass: Common ion effect. *Colloids and Surfaces A: Physicochemical and Engineering Aspects*, **387**(1–3), 43–49.

Aryal, R. L., Poudel, B. R., Pokhrel, M. R., Paudyal, H., & Ghimire, K. N. (2021). Effectiveness of Zr (IV)-Loaded Banana Peels Biomass for the Uptake of Fluoride Anion from Water. *Journal of Institute of Science and Technology*, **26**(2), 67–78.

Badamasi, H., Yaro, M. N., Ibrahim, A., & Bashir, I. A. (2019). Impacts of phosphates on water quality and aquatic life. *Chem. Res. J*, **4**, 124-133.

Hena, S., Atikah, S., & Ahmad, H. (2015). Removal of phosphate ion from water using chemically modified biomass of sugarcane bagasse. *Int. J. Eng. Sci*, **4**, 51-62.

Blaney, L., Cinar, S., & Sengupta, A. (2007). Hybrid anion exchanger for trace phosphate removal from water and wastewater. *Water Research*, **41**(7), 1603.

Breeuwsma, A., & Lyklema, J. (1973). Physical and chemical adsorption of ions in the electrical double layer on hematite (α-Fe2O3). *Journal of Colloid and Interface Science*, **43**(2), 437–448. Chakrabarti, S. (2018). *Eutrophication - A Global Aquatic Environmental Problem: A Review*.

Chen, R.-F., Liu, T., Rong, H.-W., Zhong, H.-T., & Wei, C.-H. (2021). Effect of organic substances on nutrients recovery by struvite electrochemical precipitation from synthetic anaerobically treated swine wastewater. *Membranes*, **11**(8), Article 8.

Dietary food-additive phosphate and human health outcomes. *Comprehensive reviews in food science and food safety*, **16**(5), 906-1021.

Borukhov, I., Andelman, D., & Orland, H. (1999). Effect of polyelectrolyte adsorption on intercolloidal forces. *The Journal of Physical Chemistry* B, **103**(24), 5042-5057.

El-Khaiary, M. I., & Malash, G. F. (2011). Common data analysis errors in batch adsorption studies. *Hydrometallurgy*, **105**(3–4), 314–320.

Habiby, S. R., Esmaeili, H., & Foroutan, R. (2020). Magnetically modified MgO nanoparticles as an efficient adsorbent for phosphate ions removal from wastewater. *Separation Science and Technology (Philadelphia)*, **55**(11), 1910–1921. Hill, T. L. (1952). Theory of Physical Adsorption. In W. G. Frankenburg, V. I. Komarewsky, & E. K. Rideal (Eds.), *Advances in Catalysis* (Vol. **4**, pp. 211–258).

Holtan, H., Kamp-Nielsen, L., & Stuanes, A. O. (1988). Phosphorus in soil, water and sediment: an overview. In Phosphorus in Freshwater Ecosystems: Proceedings of a Symposium held in Uppsala, *Springer Netherland*, Sweden, September **1985** (19-34).

Kılıç, Z. (2020). The importance of water and conscious use of water. *International Journal of Hydrology*, **4,** 239–241.

Lakshmipathy, R., & Sarada, N. C. (2013). Application of watermelon rind as sorbent for removal of nickel and cobalt from aqueous solution. *International Journal of Mineral Processing*, **122,** 63–65.

Li, M., Liu, J., Xu, Y., & Qian, G. (2016). Phosphate adsorption on metal oxides and metal hydroxides: A comparative review. *Environmental Reviews*, **24**(3), 319–332.

Lin, L., Yang, H., & Xu, X. (2022). Effects of water pollution on human health and disease heterogeneity: a review. *Frontiers in environmental science*, **10**, 880246.

M. Divya Jyothi. (2012). Phosphate pollution control in waste waters using new bio-sorbents. *International Journal of Water Resources and Environmental Engineering*, **4**(4).

Madhav, S., Ahamad, A., Singh, A. K., Kushawaha, J., Chauhan, J. S., Sharma, S., & Singh, P. (2020). Water pollutants: sources and impact on the environment and human health. Sensors in water pollutants monitoring: *Role of material*, 43-62.

Manna, A., Naskar, N., Sen, K., & Banerjee, K. (2022). A review on adsorption mediated phosphate removal and recovery by biomatrices. *Journal of the Indian Chemical Society*, **99**(10), 100682.

Mittal, A., Kaur, D., Malviya, A., Mittal, J., & Gupta, V. K. (2009). Adsorption studies on the removal of coloring agent phenol red from wastewater using waste materials as adsorbents. *Journal of Colloid and Interface Science*, **337**(2), 345–354.

Nagoya, S., Nakamichi, S., & Kawase, Y. (2019a). Mechanisms of phosphate removal from aqueous solution by zero-valent iron: A novel kinetic model for electrostatic adsorption, surface complexation and precipitation of phosphate under oxic conditions. *Separation and Purification Technology*, **218**, 120–129.

Panda, H., Tiadi, N., Mohanty, M., & Mohanty, C. R. (2017). Studies on adsorption behavior of an industrial waste for removal of chromium from aqueous solution. *South African Journal of Chemical Engineering*, **23**, 132–138.

Peleka, E. N., & Deliyanni, E. A. (2009a). Adsorptive removal of phosphates from aqueous solutions. *Desalination*, **245**(1–3), 357–371.

Pokhrel, M. R., Poudel, B. R., Aryal, R. L., Paudyal, H., & Ghimire, K. N. (2019a). Removal and recovery of phosphate from water and wastewater using metal-loaded agricultural waste-based adsorbents: A review. *Journal of Institute of Science and Technology*, **24**(1), 77–89.

Ren, L., Huo, H., Zhang, F., Hao, W., Xiao, L., Dong, C., & Xu, G. (2016). The components of rice and watermelon root exudates and their effects on pathogenic fungus and watermelon defense. *Plant Signaling & Behavior*, **11**(6), e1187357.

Santana, W., Ferreira, D., Rosa, F., Gustavo, L., Ruggiero, R., & Mathias, E. (2011). *Phosphate adsorption on chemically modified sugarcane bagasse fibres*. **5**, 1–7.

Saravanan, P., Josephraj, J., & Pushpa Thillainayagam, B. (2021). A comprehensive analysis of biosorptive removal of basic dyes by different biosorbents. *Environmental Nanotechnology, Monitoring & Management*, **16**, 100560.

Sartor, J. D., & Boyd, G. B. (1972). Water pollution aspects of street surface contaminants *US Government Printing Office*, (Vol. **2**).

Schaum, C. (Ed.). (2018). Phosphorus: Polluter and Resource of the Future: Motivations, Technologies and Assessment of the Elimination and Recovery of Phosphorus from Wastewater. *IWA publishing.*

Schindler, D. W., Armstrong, F. A. J., Holmgren, S. K., & Brunskill, G. J. (1971). Eutrophication of Lake 227, Experimental Lakes Area, Northwestern Ontario, by Addition of Phosphate and Nitrate. *Journal of the Fisheries Research Board of Canada*, **28**(11), 1763–1782.

Schwarzenbach, R. P., Egli, T., Hofstetter, T. B., Von Gunten, U., & Wehrli, B. (2010). Global water pollution and human health. *Annual review of environment and resources*, **35**(1), 109-136.

Shiklomanov, I. A., & Rodda, J. C. (2003). World Water Resources at the Beginning of the Twenty-First Century. *Cambridge University Press.*

Sing, K. S. W. (1998). Adsorption methods for the characterization of porous materials. *Advances in Colloid and Interface Science*, **76–77**, 3–11.

Smith, V. H., & Schindler, D. W. (2009). Eutrophication science: Where do we go from here? *Trends in Ecology & Evolution*, **24**(4), 201–207.

Ma, X., Shi, W., & Yang, H. (2022). Study on water spraying distribution to improve the energy recovery performance of indirect evaporative coolers with nozzle arrangement optimization. *Applied Energy*, **318**, 119212.

Weng, L., Van Riemsdijk, W. H., & Hiemstra, T. (2012). Factors Controlling Phosphate Interaction with Iron Oxides. *Journal of Environmental Quality*, **41**(3), 628–635.

Xiong, W., Tong, J., Yang, Z., Zeng, G., Zhou, Y., Wang, D., Song, P., Xu, R., Zhang, C., & Cheng, M. (2017). Adsorption of phosphate from aqueous solution using iron-zirconium modified activated carbon nanofiber: Performance and mechanism. *Journal of Colloid and Interface Science*, **493,** 17–23.

APPENDIX


BOROSIL


Thesis Running
Please Be Careful
Thesis Running
Please Be Careful

Adsorptive removal of phosphate anion from...

By: Sirjana Bhattarai

As of: May 31, 2024 10:33:57 AM
11,927 words - 38 matches - 9 sources

Similarity Index

8%

Mode: Summary Report

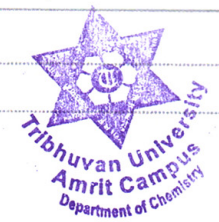

sources:

145 words / 1% - from 24-Aug-2023 12:00AM
elibrary.tucl.edu.np

100 words / 1% - from 02-Feb-2024 12:00AM
elibrary.tucl.edu.np

65 words / 1% - from 18-Apr-2023 12:00AM
elibrary.tucl.edu.np

62 words / 1% - from 18-Jan-2024 12:00AM
elibrary.tucl.edu.np

53 words / 1% - from 02-Feb-2024 12:00AM
elibrary.tucl.edu.np

126 words / 1% - from 06-Nov-2023 12:00AM
no.overleaf.com

97 words / 1% - Crossref
Ram Lochan Aryal, Khem Prasad Bhurtel, Bhoj Raj Poudel, Megh Raj Pokhrel, Hari Paudyal, Kedar Nath Ghimire. "Sequestration of phosphate from water onto modified watermelon waste loaded with Zr(IV)", Separation Science and Technology, 2021

78 words / 1% - Internet from 10-Nov-2014 12:00AM
dns2.asia.edu.tw

59 words / 1% - Internet from 09-Oct-2022 12:00AM
vdocuments.net

paper text:

ADSORPTIVE REMOVAL OF PHOSPHATE ANION FROM AQUEOUS SOLUTION USING Al(III)- LOADED SAPONIFIED WATERMELON